Polyethylene glycol (PEG)-associated immunological effects triggered by clinically relevant lipid nanoparticles

Haiyang Wang[1,2†], Yisha Wang[1,2†], Changzheng Yuan[3†], Xiao Xu[4], Wenbin Zhou[1,2], Yuhui Huang[3], Huan Lu[1,2], Yue Zheng[1,2], Gan Luo[1,2], Jia Shang[1,2], Meihua Sui[1,2*]

[1]*School of Basic Medical Sciences and Women's Hospital, Zhejiang University School of Medicine, Hangzhou, China*
[2]*Cancer Center, Zhejiang University, Hangzhou, China.*
[3]*School of Public Health, Zhejiang University School of Medicine, Hangzhou, China.*
[4]*Key Laboratory of Integrated Oncology and Intelligent Medicine of Zhejiang Province, Department of Hepatobiliary and Pancreatic Surgery, Affiliated Hangzhou First People's Hospital, Zhejiang University School of Medicine, Hangzhou, 310006, China*

†Equal contribution

***Corresponding author**
Meihua Sui, M.D., Ph.D. **E-mail:** suim@zju.edu.cn

Abstract

Polyethylene glycol (PEG)-conjugated lipid significantly contributed to the success of three approved lipid nanoparticles (LNP)-delivered therapeutics, including two COVID-19 mRNA vaccines. With the large-scale vaccination of mRNA vaccines, it has become an imminent task to elucidate the possible PEG-associated immune responses induced by clinically relevant LNP. Up to date there are only four small-scale population-based studies emphasizing the changes of PEG-specific antibodies upon injection of mRNA vaccines. However, inconsistent data were obtained due to significant person-to-person and study-to-study variabilities. To clarify the PEG-associated immune responses triggered by clinically relevant LNP in a model system with least "noise", we initiated an animal study using the PEGylated LNP of BNT162b2 (with the largest number of recipients) as a representative LNP and simulated the clinical practice. Through designing a series of time points and three doses correlated with the PEG exposure amount contained in three approved LNP-based drugs, we demonstrated for the first time that generation and changes of anti-PEG IgM and IgG were time- and dose-dependent. Unexpectedly, we found that unlike other thymus-independent antigens (TI-Ag), PEGylated LNP not only induced isotype switch and production of anti-PEG IgG, but caused immune memory, leading to rapid enhancement and longer lasting time of both anti-PEG IgM and IgG upon repeated injection. Importantly, pharmacokinetic studies discovered that initial injection of PEGylated LNP accelerated the blood clearance of subsequently injected LNP. These findings refine our understandings on PEGylated LNP and possibly other PEG derivatives, and may lead to optimization of premarket guidelines and clinical practice of PEGylated LNP-delivered therapeutics.

Introduction

Development of nucleic acid therapeutics has been restricted by the intrinsic defects of nucleic acids such as poor stability, immunogenicity and low penetration capability through cell membranes. Therefore, delivery platform possessing high stability, good targeting affinity and strong cellular internalization are urgently needed for therapeutic nucleic acids (*1*). Among various delivery systems for nucleic acids, lipid nanoparticles (LNP), which have four components including ionizable cationic lipid, cholesterol, 1,2-distearoyl-sn-glycero-3-phosphocholine (DSPC) and polyethylene glycol (PEG)-conjugated lipid (*2*), are of greatest attention due to unique advantages such as simple formulation, good biocompatibility, large payload and low toxic side effects (*3*). So far, there are three FDA-approved nucleic acid drugs using LNP as delivery vectors, namely Onpattro® (Patisiran, approved on August 10, 2018, an siRNA drug), the first COVID-19 mRNA vaccine Comirnaty® (BNT162b2, emergency use authorization approved on December 2, 2020) and the second COVID-19 mRNA vaccine Spikevax® (mRNA-1273, emergency use authorization approved on December 18, 2020) (*4*).

It has been demonstrated that modification of therapeutics with PEG, so called “PEGylation”, has multiple advantages such as increasing drug solubility and stability, reducing unfavorable immunogenicity and extending drug half-life (*5*). Indeed, as the first approved vaccine using PEG as an excipient, its PEG-conjugated lipid (ALC-0159) plays critical roles in improving the stability and prolonging blood circulation of LNP, which has significantly contributed to the overwhelming success of BNT162b2 in clinical trials (*6*). There used to be a general perception that PEG and its derivatives were nonimmunogenic. However, since anti-PEG IgM was first detected in rabbits immunized with PEGylated ovalbumin in 1983 (*7*), an expanding body of evidence has revealed that some PEG derivatives could elicit PEG-specific antibodies (*8-10*). Subsequently, anti-PEG antibodies may form "antigen-antibody" complexes with newly injected PEGylated agents. As a result, the immune complexes may be cleared by macrophage Fc receptor-mediated and complement receptor-mediated phagocytosis, leading to changes in the pharmacokinetics of newly injected PEGylated therapeutics and reduction of the drug efficacy (*8-11*). For instance, Dr. Roffler first demonstrated that anti-PEG IgM quickly cleared PEG-modified proteins from the blood in mice in 1999 (*12*). Later, Ishida T *et al.* proved that anti-PEG IgM elicited by an initial exposure to PEGylated liposomes triggered the accelerated blood clearance (ABC phenomenon) of subsequently administrated liposomes in rats *via* activation of the complement system (*13*). There are even clinical investigations demonstrating accelerated clearance of drugs triggered by anti-PEG antibodies and reduction of therapeutic efficacy (*14, 15*).

With the large-scale vaccination of mRNA vaccine and the development of therapeutics using LNP as carriers, it has become an imminent task to elucidate the potential PEG-associated immunological effects induced by clinically relevant LNP. However, up to date there are only four related literatures, all of which are recent clinical observations including three reports based on mRNA vaccines: Alnylam Pharmaceuticals *Inc.* reported that anti-PEG IgM and IgG were induced in 3.4% of subjects (5 out of 145 patients) who received Patisiran in 2019 (*16*); Kent *et al.*

reported on June 27, 2022 that COVID-19 mRNA vaccines boosted the serum anti-PEG antibody levels in Australian recipients, with anti-PEG IgM boosted a mean of 2.64 folds and anti-PEG IgG boosted a mean of 1.78 folds following BNT162b2 vaccination (n=55), as well as anti-PEG IgM boosted a mean of 68.5 folds and anti-PEG IgG boosted a mean of 13.1 folds following mRNA-1273 vaccination (n=20) (*17*); Calzolai *et al.* from Joint Research Centre in Italy reported a significant increase in anti-PEG IgM level after the first injection of BNT162b2 and the third injection of BNT162b2 or mRNA-1273, while no boosting effect was observed on anti-PEG IgG after injection with either vaccine on August 9, 2022 (*18*); Krammer *et al* reported different response on induction of PEG-specific antibodies with a very small size of recipients in USA received either BNT162b2 or mRNA-1273 vaccination (n=10) on September 14, 2022 (*19*). It is noteworthy that as stated by the authors, pre-existing antibodies, small population sizes and inevitable interference due to exposure to PEG-containing substances other than vaccines after immunization may compromise the accuracy of clinical data, which may be responsible for the inconsistent results (*17*, *19*). Moreover, the amount of mPEG2000 contained in each single injection varies significantly among the three FDA-approved LNP-delivered therapeutics (*20-22*). For instance, mPEG2000 contained in each injection of ONPATTRO is as high as 262 times of that in BNT162b2 (*20*), which has raised our concern on the potential impact of exposure amount over PEG-associated immunological effect induced by LNP. Another important aspect is that as the first vaccine using PEG as an excipient and LNP as a carrier, the *in vivo* pharmacokinetics of COVID-19 mRNA vaccine might differ from all other vaccines previously approved for clinical use, considering that the *in vivo* process of mRNA vaccine is mainly determined by its LNP vector (*21*). Unfortunately, until now there is still a lack of pharmacokinetic data of both BNT162b2 and mRNA-1273.

Motivated by these questions, we herein successfully synthesized the PEGylated LNP of BNT162b2, the most widely used LNP-delivered therapeutic, as a model LNP. DiR-labeled LNP (DiR@LNP) and DiR-labeled LNP encapsulating mRNA encoding the firefly luciferase (DiR-LU@LNP) were also prepared for visualization and *in vivo* quantitative studies. A Wistar rat model was selected, in order to take the advantage of well controlled animal studies to eliminate undesired exposure to PEG and its derivatives other than PEGylated LNP. Through simulating the clinical application of BNT162b2, *e.g.* two intramuscular injections with an interval of 21 days, we carefully characterized the model LNP in inducing PEG-associated immunological effects, *e.g.* dynamic changes in the subtypes and levels of anti-PEG antibodies. Importantly, three clinically relevant doses covering the whole range of PEG contained in a single injection of three FDA-approved LNP-delivered therapeutics, were delicately designed and studied, in order to assess the impact of PEG exposure amount on induction of anti-PEG antibodies. Moreover, potential pharmacokinetic changes caused by anti-PEG antibodies following repeated injection of PEGylated LNP were explored for the first time.

Results

Successful synthesis and physiochemical characterization of PEGylated LNP, DiR-LNP and DiR-LU@LNP

As shown in Fig. 1A and Fig. 1B, as well as described in “Methods”, LNP, DiR-LNP and DiR-LU@LNP were prepared by mixing of the ethanol phase (ALC-0315, DSPC, cholesterol and ALC-0159 in ethanol, with or without DiR) and the aqueous phase (citrate buffer with or without firefly luciferase mRNA) through a microfluidic mixing device. The obtained LNP formulations were first examined with Cryo-TEM, in which both LNP and DiR-LNP were hollow spheres, while DiR-LU@LNP had a typical electron-dense core structure containing mRNA (Fig. 1C). Next, LNP formulations were characterized with their Z-average (in neutral PBS), PDI (in neutral PBS) and surface Zeta potential (in ultrapure water) using DLS. As shown in Fig. 2A-2B and table S1, the Z-average/PDI/Zeta potential of LNP, DiR-LNP and DiR-LU@LNP were 110.400 ± 3.466 nm/0.203 ± 0.012/16.733 ± 0.451 mV, 113.067 ± 2.139 nm/0.183 ± 0.013/7.257 ± 0.168 mV and 101.367 ± 2.593 nm/0.197 ± 0.015/-5.943 ± 0.129 mV, respectively. These data demonstrate that all three types of LNP formulations have favorable particle diameter (around 100-110 nm), highly monodisperse particle-size distribution (PDI<0.3), and weak surface charge (-5.943 mV~+ 16.733 mV) (*23*, *24*).

As depicted in Fig. 2C and fig. S1, the Z-average/PDI of LNP formulations at four time points were as follows: LNP, 140.533 ± 2.768 nm/0.264 ± 0.012, 138.600 ± 0.100 nm/0.274 ± 0.005, 138.200 ± 0.954 nm/0.287 ± 0.013 and 141.867 ± 2.631 nm/0.287 ± 0.016 (Fig. 2C and fig. S1); DiR-LNP, 104.300 ± 0.458 nm/0.285 ± 0.014, 105.733 ± 0.503 nm/0.282 ± 0.010, 107.267 ± 1.940 nm/0.291 ± 0.013 and 117.200 ± 1.277 nm/0.392 ± 0.020 (Fig. 2D and fig. S2); DiR-LU@LNP, 135.067 ± 1.550 nm/0.240 ± 0.003, 133.867 ± 0.058 nm/0.251 ± 0.001, 132.667 ± 2.023 nm/0.246 ± 0.006 and 134.133 ± 1.222 nm/0.252 ± 0.006 (Fig. 2E and fig. S3). These data suggest that LNP, DiR-LNP and DiR-LU@LNP nanoparticles have relatively stable particle sizes and stay monodisperse *in vivo*.

Moreover, as the phospholipid component in LNP is commonly used for determining the amount of whole nanoparticles (*25*, *26*), the standard curves of phospholipid (DSPC) in LNP, DiR-LNP and DiR-LU@LNP were respectively drawn and the following equations were obtained, in which y represents absorbance measured at 470 nm and x represents phospholipid concentration: y=0.0077x+0.0098 (R^2=0.9914; Fig. 2F); y=0.0076x+0.0244 (R^2=0.9909; Fig. 2G); y= 0.0071x+0.0284 (R^2 = 0.9841; Fig. 2H). These equations were used for subsequent calculation of three clinically relevant doses of LNP including low dose (L-LNP, 0.009 mg phospholipids/kg), middle dose (M-LNP, 0.342 mg phospholipids/kg) and high dose (H-LNP, 2.358 mg phospholipids/kg) (see “Methods”).

Time- and dose-dependent induction of anti-PEG IgM antibody by PEGylated LNP

As shown in the schematic illustration (Fig. 3A), Wistar rats were respectively administered with two intramuscular injections of LNP at above-mentioned three doses on Day 0 and Day 21 (simulating the clinical schedule of BNT162b2). Subsequently, serum samples were collected at

12 designated time points (Day 0, 3, 5, 7, 14, 21, 24, 26, 28, 35, 42 and 49) and examined for the presence and level of anti-PEG IgM with ELISA. The obtained data were summarized in Fig. 3B, with statistical analysis conducted among control, L-LNP, M-LNP and H-LNP groups for each time point.

Our data indicated that anti-PEG IgM was initially detected in L-LNP group on Day 3 after the first injection. Impressively, although the serum anti-PEG IgM was not detectable until Day 5 after the first injection of M-LNP and H-LNP, the initial antibody levels induced by these two LNP doses were significantly higher than that induced by L-LNP (P<0.001, L-LNP *vs* M-LNP; P< 0.0001, L-LNP *vs* H-LNP). Another finding is that during the first injection cycle (Day 0~21), L-LNP transiently induced anti-PEG IgM only detectable on Day 3 and Day 5, while M-LNP and H-LNP induced more persistent and higher levels of anti-PEG IgM detectable on Day 5, 7, 14 and 21. These data suggest that an initial single injection of PEGylated LNP induced both time- and dose-dependent induction of anti-PEG IgM. Interestingly, anti-PEG IgM was detected at more time points for all LNP doses after the second injection. For instance, there were 4 anti-PEG IgM-detectable time points (Day 24, 26, 28 and 35) in LNP group after the second injection, while there were only 2 anti-PEG IgM-detectable time points (Day 3 and Day 5) during the first injection cycle. M-LNP and H-LNP even constantly induced anti-PEG IgM throughout the whole second injection cycle (Day 21~42) and the extension period (Day 42~49). In addition, there was statistical significance among different groups/doses on the level of anti-PEG IgM, which was ranked as follows: H-LNP>M-LNP>L-LNP at all detectable time points including Day 24, 26, 28 and 35. These data provided additional evidence for the dose- and time-dependency of anti-PEG IgM induced by PEGylated LNP. Further calculation and comparison showed that the peak levels of anti-PEG IgM induced by the second injection of LNP were higher than those induced by the first injection at the same dose: L-LNP, 2.374 on Day 28 *vs* 1.996 on Day 5; M-LNP, 3.692 on Day 26 *vs* 2.704 on Day 5; H-LNP, 4.262 on Day 26 *vs* 2.492 on Day 5. Herein, we would like to emphasize that the high ELISA assay precision, as indicated by the very low variation of standards (CV%=3.365 ± 2.934%) and samples (CV%=4.342 ± 5.510%), as well as the high average linear regression coefficient of determination of standard curves (R^2=0.985 ± 0.005), demonstrated that our ELISA assays for anti-PEG IgM had good quality control and the obtained data were reliable (Fig. 3C).

As indicated by plotted curves (Fig. 3D), profile analysis found that time-courses of anti-PEG IgM production between every two groups showed different profiles. Furthermore, changes over time (12 time points) and differences across groups (3 doses) regarding LNP-induced anti-PEG IgM were evaluated for statistical significance using linear mixed model analysis. As indicated by corresponding statistical analysis (Table 1), β for "Group", which represented differences on antibody level among various groups at all time points, exhibited statistical significance between Control *vs* M-LNP (P<0.0001), Control *vs* H-LNP (P=0.0035) and L-LNP *vs* M-LNP (P=0.0011). Significant differences were also detected with β for "Time" (P=0.0116) and "Time^2" (P<0.0001), both of which represent rate of change in antibody level

over time (12 time points). Regarding β for "Group*Time", which represented mean differences in the rate of change in antibody level over time among various groups, we found that compared with the Control group, both M-LNP and H-LNP groups had faster rates of anti-PEG IgM production (β for M-LNP*Time: 0.0238 [0.0167, 0.0308] higher per day, β for H-LNP*Time: 0.0458 [0.0387, 0.0528] higher per day, both $P<0.0001$ *vs* Control*Time), while the change rate of L-LNP group was similar to the Control group (β for L-LNP*Time: 0.0034 [-0.0036, 0.0105] higher per day, $P=0.3408$ *vs* Control*Time). Particularly, H-LNP group exhibited the fastest rate in anti-PEG IgM production among the four groups (H-LNP*Time *vs* L-LNP*Time, H-LNP*Time *vs* M-LNP*Time, M-LNP*Time *vs* L-LNP*Time, all $P<0.0001$). These data have provided additional evidence for dose- and time- dependent induction of anti-PEG IgM by PEGylated LNP. Another interesting finding discovered by linear mixed model analysis was the significant difference on antibody level between the first and second injections (β for "Second Injection": 0.9166 [0.7852, 1.0479], $P<0.0001$ *vs* First Injection), which coincides with the longer lasting period and higher level of anti-PEG IgM induced by repeated injection of LNP compared with the initial injection (Fig.3, B and D).

Time- and dose-dependent induction of anti-PEG IgG antibody by PEGylated LNP

Serum samples collected at above-mentioned 12 time points were further examined for the presence and level of anti-PEG IgG with ELISA. The obtained data were summarized in Fig. 4A, with a high ELISA assay precision demonstrated by the very low variation of standards (CV%=3.472 ± 3.634%) and samples (CV%=4.545 ± 7.867), as well as the high average linear regression coefficient of determination of standard curves (R^2=0.999 ± 0.001) (Fig. 4B). Different from the characteristics of LNP in inducing anti-PEG IgM (Fig. 3), no anti-PEG IgG was detected throughout the first injection cycle in all experimental groups (Day 0~21). These data demonstrate that an initial single injection of PEGylated LNP, at a broad range of doses tested in this study, did not induce anti-PEG IgG antibody in Wistar rats. Interestingly, although anti-PEG IgG was still not detectable after the second injection of L-LNP (Day 21~49), it was clearly induced by a repeated injection of M-LNP and H-LNP, and constantly existed at all later time points tested (Day 24~49). Similar to the findings with anti-PEG IgM, anti-PEG IgG levels induced by H-LNP were significantly higher than those induced by M-LNP at all detectable time points, demonstrating a dose-dependency on anti-PEG IgG induced by PEGylated LNP. In particular, the anti-PEG IgG levels increased to the peaks on Day 26 in both M-LNP and H-LNP groups (2.083 ± 0.306 and 2.547 ± 0.247, respectively, Fig. 4, A and C). Another point worthy of note is that anti-PEG IgM levels induced by LNP were generally higher than the corresponding values of anti-PEG IgG.

As indicated by plotted curves (Fig. 3C), profile analysis found that time-courses of anti-PEG IgG production in the control and L-LNP groups had equal levels whereas other comparisons of time-courses between every two groups showed different profiles. Linear mixed model analysis was further conducted to evaluate the statistical significance on changes of LNP-

induced anti-PEG IgG over time (12 time points) and differences across groups (3 doses). As indicated by corresponding statistical analysis (Table 2), β for "Group", which represented differences on antibody level among various groups at all time points, exhibited statistical significance between M-LNP *vs* L-LNP (P=0.0195), H-LNP *vs* L-LNP (P=0.0054). Significant differences were also detected with β for "Time" (P=0.0077) and "Time^2" (P=0.0197), both of which represent rate of change in antibody level over time (12 time points). Regarding β for "Group*Time", which represented mean differences in the rate of change in antibody level over time among various groups, we found that compared with the Control group, both M-LNP and H-LNP groups had faster rates of anti-PEG IgG production (β for M-LNP*Time: 0.0149 [0.0105, 0.0193] higher per day, β for H-LNP*Time: 0.0244 [0.0200, 0.0288] higher per day, both P<0.0001 *vs* Control*Time), while the change rate of L-LNP group was similar to the Control group (β for L-LNP*Time: 0.0011 [-0.0033, 0.0054] higher per day, P=0.6339 *vs* Control*Time). Particularly, H-LNP group exhibited the fastest rate in anti-PEG IgG production among the four groups (H-LNP*Time *vs* L-LNP*Time, H-LNP*Time *vs* M-LNP*Time, M-LNP*Time *vs* L-LNP*Time, all P<0.0001). These data have provided additional evidence for dose- and time-dependent induction of anti-PEG IgG by PEGylated LNP. Another interesting finding discovered by linear mixed model analysis was the significant difference on antibody level between the first and second injections (β for "Second Injection": 0.6549 [0.5734, 0.7364], P<0.0001 *vs* First Injection) (Fig.4, A and C).

Enhanced production of anti-PEG antibodies by previous exposure to PEGylated LNP

To evaluate the potential influence of previous exposure to PEGylated LNP on the production of anti-PEG IgM and IgG antibodies after subsequent exposure to same LNP, increased anti-PEG IgM (▲Anti-PEG IgM (Log_{10} CONC)) and increased anti-PEG IgG production (▲Anti-PEG IgG (Log_{10} CONC)) were respectively calculated by subtracting log10-transformed anti-PEG antibody concentration determined by quantitative ELISA assay after first injection (Anti-PEG IgM (Log_{10} $CONC_{1st\ injection}$) or Anti-PEG IgG (Log_{10} $CONC_{1st\ injection}$)) from log10-transformed antibody concentration determined after the second injection (Anti-PEG IgM (Log_{10} $CONC_{2nd\ injection}$) or Anti-PEG IgG (Log_{10} $CONC_{2nd\ injection}$)) at corresponding 3 doses and 6 time points (Day 0, 3, 5, 7, 14 and 21). The obtained data were summarized in Fig. 5 (A and B for ▲Anti-PEG IgM (Log_{10} CONC), C and D for ▲Anti-PEG IgG (Log_{10} CONC)). As introduced in Fig. 5B, profile analysis found that time-courses of enhanced anti-PEG IgM production (▲Anti-PEG IgM (Log10 CONC)) between every two groups showed different profiles.

As indicated in Fig. 5A, although ▲Anti-PEG IgM (Log_{10} CONC) was not detectable until Day 5 in L-LNP group, increased anti-PEG IgM production was observed at all the time points in both M-LNP and H-LNP groups. Moreover, two sequential injections of L-LNP only induced transient ▲Anti-PEG IgM (Log_{10} CONC) detectable on Day 5, 7 and 14, while those of M-LNP and L-LNP induced more persistent and higher level of ▲Anti-PEG IgM (Log_{10} CONC)

detectable on Day 3, 5, 7, 14 and 21. In particular, the peak levels of ▲Anti-PEG IgM (Log_{10} CONC) induced by different doses of PEGylated LNP were 0.654 ± 0.471 (L-LNP, Day 7), 1.574 ± 0.399 (M-LNP, Day 3) and 2.277 ± 0.410 (H-LNP, Day 3), respectively (Fig. 5, A and B). Importantly, by using linear mixed model analysis, we further demonstrated the statistical significance on changes over 6 time points and differences across groups (3 doses) regarding LNP-induced ▲Anti-PEG IgM (Log_{10} CONC) (Fig. 5, A and B; Table 3). For instance, the dose dependency of enhanced production of anti-PEG IgM was confirmed, as ▲Anti-PEG IgM (Log_{10} CONC) ranking from high to low was that respectively induced by H-LNP, M-LNP and L-LNP at all detectable time points, with significant difference among these three groups (P<0.0001 for M-LNP *vs* L-LNP and H-LNP vs L-LNP; P=0.0003 for H-LNP *vs* M-LNP). Moreover, rate of change in ▲Anti-PEG IgM (Log_{10} CONC) over 6 time points also exhibited significant differences, with P<0.0001 for both "Time" and "$Time^2$". Regarding β for "Group*Time", which represented mean differences in the rate of change in ▲Anti-PEG IgM (Log_{10} CONC) over time among various groups, we found that compared with the L-LNP group, both M-LNP and H-LNP groups had faster rates of ▲Anti-PEG IgM (Log_{10} CONC) (P=0.0138, M-LNP*Time *vs* L-LNP*Time; P=0.0149, H-LNP*Time *vs* L-LNP*Time). These data have provided additional evidence for dose- and time- dependency of ▲Anti-PEG IgM (Log_{10} CONC) induced by two sequential injections of PEGylated LNP.

Furthermore, quantification of increased anti-PEG IgG production (▲Anti-PEG IgG (Log_{10} CONC)) was summarized in Fig. 5C, with time-course profiles of ▲Anti-PEG IgG (Log_{10} CONC) across four groups plotted in Fig. 5D and linear mixed model analysis summarized in Table 4. As introduced in Fig. 5D, profile analysis found that time-courses of enhanced anti-PEG IgG production (▲Anti-PEG IgG (Log_{10} CONC)) in the control and L-LNP groups were also equivalent whereas other comparisons of time-courses between every two groups showed different profiles. Our data showed that ▲Anti-PEG IgG (Log_{10} CONC) was not detectable in L-LNP group at all time points. Nor was it detectable on Day 0 of L-LNP, M-LNP or H-LNP groups. However, ▲Anti-PEG IgG (Log_{10} CONC) was detected at all later time points (Day 3, 5, 7, 14 and 21) in both M-LNP and H-LNP groups, with peak levels induced on Day 5 (0.888 ± 0.459) and Day 7 (1.354 ± 0.308), respectively (Fig. 5, A and B). Moreover, statistical significance was observed between various groups including Control *vs* M-LNP, Control *vs* H-LNP, L-LNP *vs* M-LNP, L-LNP *vs* H-LNP and M-LNP *vs* H-LNP. Consistent with these data, Control and L-LNP groups exhibited quite similar time-course profile of ▲Anti-PEG IgG (Log_{10} CONC), whereas there was significant difference among profiles of Control/L-LNP, M-LNP and H-LNP groups (Fig. 5B). Indeed, data introduced in Table 4 further confirmed these findings, as ▲Anti-PEG IgG (Log_{10} CONC) ranking from high to low was that respectively induced by H-LNP, M-LNP and L-LNP at all detectable time points, with significant difference among these three groups (β for L-LNP: 0.0149 [-0.1866, 0.2164], β for M-LNP: 0.5180 [0.3165, 0.7195]; β for H-LNP: 0.8861 [0.6846, 1.0876]; P<0.0001, comparisons between any two groups). Together with the significant

differences on rate of change in ▲Anti-PEG IgG (Log_{10} CONC) over 6 time points (P<0.0001 for both "Time" and "$Time^2$"), our data clearly demonstrated that initial injection of PEGylated LNP dose- and time-dependently boosted the generation of anti-PEG IgM and IgG after the second injection.

Dose-dependent biodistribution of PEGylated LNP administered at clinically relevant doses

By using a fluorescence and bioluminescence double-labeling strategy, the biodistribution of LNP was determined in rats treated with DiR-LU@LNP simulating clinical practice (Fig. 6A). Consistent with the preclinical biodistribution data published in Assessment Report of Comirnaty®/BNT162b2 issued by the European Medicines Agency, weak bioluminescence signal of luciferase was detected in muscle at injection site and liver (fig. S4), demonstrating that DiR-LU@LNP drained into the liver and delivered active luciferase mRNA. As DiR fluorescence exhibited significantly higher sensitivity than luciferase bioluminescence (Fig. 6B and fig. S4), LNP biodistribution was further analyzed based on DiR fluorescence. Our data showed that 6 hours after both the first and second injections, DiR fluorescence was only detectable in muscle at the injection site in L-LNP group. Upon increase of LNP dose, the fluorescent signal was significantly enhanced and detected in more organs/tissues (muscle at the injection site, liver and lung in M-LNP group; muscle at the injection site, liver, lung, spleen and draining lymph node in H-LNP group). Further analysis indicated that the total radiant efficiency from liver, lung, spleen and heart exhibited statistical significance between Control *vs* M-LNP, Control *vs* H-LNP, L-LNP *vs* M-LNP, L-LNP *vs* H-LNP, and M-LNP *vs* H-LNP after both the first and second injections. These findings demonstrate a dose-dependent biodistribution of LNP, with preferential accumulation in reticuloendothelial system after entering the blood circulation *via* intramuscular injection (Fig. 6, B and C).

Blood clearance of PEGylated LNP administered at three clinically relevant doses simulating clinical schedule

To explore whether previous exposure to PEGylated LNP would alter the pharmacokinetic of newly or repeatedly injected LNP, Wistar rats were administered with two intramuscular injections with DiR-labeled LNP (DiR-LNP) at above-mentioned doses and schedule (Fig. 7A and "Methods"). After each injection, serum samples were respectively collected at a series of designated time points including 5 minutes, 30 minutes, 1 hour, 3 hours, 6 hours, 10 hours, 24 hours and 48 hours for further measurement of DiR fluorescence intensity with a SpectraMax® iD5 multi-mode microplate reader. As shown in Fig. 7B, LNP-associated DiR fluorescence was not detectable in serums collected from L-LNP group at all time points after both injections, indicating the extremely low level of LNP in blood circulation of rats administered with low dose of DiR-LNP. However, significantly increased DiR fluorescence was observed in serums isolated from M-LNP (at 6 hours and 10 hours) and H-LNP (at 7 sequential time points ranging from 30

minutes till 48 hours) groups after an initial exposure to DiR-LNP. These data coincide with the above-mentioned dose-dependent induction of anti-PEG antibodies by LNP administered at same clinically relevant doses simulating clinical schedule. Interestingly, compared with the first injection, DiR fluorescence was detected at less time points in M-LNP (only 6 hours) and H-LNP (4 sequential time points ranging from 6 hours till 48 hours) groups after the second injection of DiR-LNP, suggesting faster blood clearance and/or reduced serum level of PEGylated LNP upon repeated exposures. Indeed, as depicted in Fig. 7C and Fig. 7D, although no statistical difference on LNP-associated fluorescence intensity was observed between two separate injections in Control, L-LNP and M-LNP groups, DiR fluorescence was significantly decreased at 30 minutes ($P<0.01$), 1 hour ($P<0.05$) and 48 hours ($P<0.05$) after repeated injection of high-dose DiR-LNP in comparison with that after the initial injection. For the first time, these data demonstrate an accelerated blood clearance phenomenon of clinically relevant PEGylated LNP triggered by previous exposure to the same LNP.

Discussion

PEG is a versatile polymer commonly used as a surfactant, solvent and emulsifying agent in household chemicals, as an additive in foods, and as either an active composition or an inactive excipient in medicine (*27*). Taking the multiple advantages of modifying therapeutics with PEG (PEGylation), FDA has approved 33 PEGylated agents for a variety of clinical indications such as metabolic disease, immunological disease, degenerative disease, cancer and infectious diseases (https://www.drugs.com). Although free PEG is poorly immunogenic and doesn't effectively elicit anti-PEG antibody response, it may acquire immunogenic properties, e.g. inducing anti-PEG antibodies, upon conjugation with other materials such as proteins and nanocarriers *(27, 28)*. Therefore, PEG is considered to be a polyvalent hapten (*28*). Interestingly, a proportion of individuals who never received PEGylated drugs have anti-PEG antibodies due to environmental exposure (*8*). For instance, an epidemiological study based on 1504 healthy Han Chinese donors residing in Taiwan area of China found that a total of 666 individuals (44.3%) had positive anti-PEG IgG or IgM, with 25.7%, 27.1%, and 8.4% of the total population having anti-PEG IgG only, anti-PEG IgM only, and both anti-PEG IgG and IgM, respectively (*29*). This study also showed that PEG-specific antibodies were more common in females than in males (32.0% vs 22.2% for IgM and 28.3% vs 23.0% for IgG), and in young people (up to 60% for 20 years old) as compared to old people (20% for>50 years old). Another epidemiological study based on 377 healthy human blood donors in USA found that anti-PEG antibodies were detectable in ~72% of individuals, with 18%, 25% and 30% of all samples having anti-PEG IgG only, anti-PEG IgM only, and both anti-PEG IgG and IgM, respectively (*30*). Importantly, anti-PEG antibodies could form "antigen-antibody" complexes with newly administered PEGylated nanocarriers/proteins, leading to biodistribution/pharmacokinetic changes of PEGylated drugs and reduced therapeutic efficacy (*8, 27*). Moreover, they may induce severe side effects such as hypersensitivity reactions of PEGylated therapeutics, although the underlying mechanisms have not been fully clarified (*27,*

31).

In the past five years, three PEGylated LNP-delivered drugs have been marketed, including Patisiran, BNT162b2 and mRNA-1273. As the first two vaccines using PEG as an excipient and/or using LNP as a carrier, BNT162b2 and mRNA-1273 essentially represent a new class of vaccines, because their biodistribution and pharmacokinetics are mainly determined by the characteristics of their nanocarrier, e.g. the PEGylated LNP prepared in this study. Unfortunately, in spite of these significant differences from traditional vaccines, no pharmacokinetic data are available for either PEGylated LNP or two LNP-delivered mRNA vaccines, as currently these data are not regularly required by WHO for market approval of intramuscular vaccines (*32*). Considering that the worldwide sales volume of BNT162b2 and mRNA-1273 has respectively reached as huge as >5,341,276,760 and >3,229,743,423 doses (public information from WHO), it is urgent to reveal the properties of PEGylated LNP in inducing PEG-related immunological effects, e.g. production of PEG-specific antibodies and subsequent influence on the pharmacokinetic of newly/repeatedly injected LNP, as these characteristics may directly affect the immune protective efficacy of both vaccines. Furthermore, clarification of these issues will provide valuable information for the research and development of a number of vaccine candidates using PEGylated LNP as a carrier (public information from WHO).

Up to date there are four published clinical investigations in total that evaluated the induction of PEG-specific antibodies by LNP-delivered drugs, including three related with BNT162b2, mRNA-1273 and mixed use of these two vaccines (*16-19*). Unfortunately, it is extremely and practically difficult to obtain reliable data with clinical studies. One major reason is the significant variability of pre-existing PEG-specific antibodies, leading to unfavorable intervention when identifying and analyzing antibodies induced by PEGylated LNP. Alnylam Pharmaceuticals Inc. reported that only two of 224 patients (0.89%) with hereditary transthyretin-mediated (hATTR) amyloidosis were positive for anti-PEG antibodies at baseline (*16*), while Kent et al from the University of Melbourne stated that anti-PEG IgG was commonly detectable (71%) before vaccination in BNT162b2 and mRNA-1273 cohorts (*17*). Calzolai et al from Joint Research Centre in Italy described that anti-PEG IgG was positive before the first vaccine injection in their cohorts receiving two LNP-based COVID-19 vaccines, with a large person-to-person variability (*18*). Another big concern is that additional exposure to PEG derivatives other than PEGylated LNP may exist during clinical observation period, which may interfere with the immunological effects induced by injected LNP. In agreement with this concern, Kent et al showed that 5 unvaccinated control donors had increased level of anti-PEG IgG, and 8 control donors had elevated anti-PEG IgM (*17*). Moreover, insufficient/very small population size, broad age range, gender-related influence, significant deviation of time points even within the same cohort, and crosstalk between BNT162b2 and mRNA-1273 upon mixed use, were additional shortcomings commonly existed in related literatures. As a result, till now no consistent evidence has been obtained regarding any characteristic of initial and/or repeated injections of either BNT162b2 or mRNA-1273 in inducing PEG-specific antibodies. Besides, the fold changes of both anti-PEG

IgM and IgG induced by either mRNA vaccine had a very broad range, further demonstrating the remarkable person-to-person variability in clinical studies.

In order to clarify the cause-and-effect relationships of clinically relevant PEGylated LNP on the induction of PEG-associated immunological effects, we herein initiated the first animal study by using the PEGylated LNP of BNT162b2, which has the largest number of recipients all over the world, and simulating its clinical practice as a representative model system. As expected, neither anti-PEG IgM (Fig. 3, B and D) nor anti-PEG IgG (Fig. 4, A and C) was detected in all experimental groups on Day 0 before initial injection of PEGylated LNP. Nor did any type of anti-PEG antibodies exist in control group throughout the whole study period (Day 0-49) (Fig. 3, B and D; Fig. 4, A and C). These data demonstrate a “clean” background and no additional “cause” other than injected LNP in our model system. Meanwhile, the shortcomings existed in clinical studies, e.g. insufficient group size, deviations on time points, as well as age- and gender-associated interferences, were easily resolved in this study. Encouragingly, through designing a series of time points and three doses respectively correlated with the amount of PEG contained in three LNP-based drugs in market (Fig. 3A), we carefully investigated the potential time- and dose-dependency of clinically relevant LNP in inducing anti-PEG antibodies. Our data clearly demonstrated that generation and changes of both anti-PEG IgM (Fig. 3, B and D; Table 1) and anti-PEG IgG (Fig. 4, A and C; Table 2) were time-dependent. In brief, anti-PEG IgM emerged on Day 3, reached the peak level on Day 5 and then gradually reduced during the first injection cycle (Day 0~21), followed by a further boosted peak on Day 26-28 after the second injection of LNP on Day 21 (Fig. 3, B and D; Fig. 5, A and B). Despite of the absence throughout the first injection cycle (Day 0~21), anti-PEG IgG emerged on Day 24 after the second injection of LNP on Day 21, and reached its peak on Day 26 (Fig. 4, A and C; Fig. 5, C and D). Meanwhile, utilization of three doses (1:38:262) essentially simulating the corresponding amount of PEG contained in a single injection of BNT162b2, mRNA-1273 and Patisiran revealed the dose dependency of LNP in inducing anti-PEG antibodies. Specifically, the amount of PEGylated LNP injected was positively correlated with the generation and serum level of anti-PEG antibodies (Fig. 3D and Fig. 4C).

Further investigation on the biodistribution of PEGylated LNP demonstrated that in addition to muscle at the injection site, LNP mainly accumulated in reticuloendothelial system such as liver, lung, spleen and draining lymph node (Fig. 6, B and C), which is essentially consistent with the biodistribution data described in the Public Assessment Report of BNT162b2 and mRNA-1273 (*33*,*34*). Importantly, we discovered that initial injection of LNP promoted the blood clearance of subsequently administered LNP (Fig. 7, C and D). To our best knowledge, this is the first study on the pharmacokinetics of two LNP-based COVID-19 vaccines or their PEGylated LNP carriers. It is noteworthy that although previously Alnylam Pharmaceuticals Inc. reported that ABC phenomenon was absent after repeated injection of Onpattro, all patients with hATTR amyloidosis in their study received corticosteroid premedication prior to each Onpattro injection to reduce the risk of infusion-related reactions (*16*). However, corticosteroid is generally considered as an immunosuppressive drug and may repress PEG-associated immunological

effects including “antigen-antibody” immune complex-mediated ABC phenomenon. Our findings on the ABC phenomenon of PEGylated LNP, together with further in-depth pharmacokinetic studies on LNP or LNP-based therapeutics, may lead to optimization of the guidelines/premarket requirements for research and development of biomedical products using PEGylated LNP as delivery vectors. For instance, preclinical pharmacokinetic studies might be necessary and important before market approval of vaccines or other drugs delivered intramuscularly using LNP.

Finally, our model system has provided an opportunity to explore the mechanisms mediating the generation of anti-PEG antibodies induced by clinically relevant PEGylated LNP (fig. S5). It is well known that non-protein antigens, such as lipids, polysaccharides, and naturally occurring non-proteinatious and synthetic polymers, can stimulate antibody response in the absence of T helper cell and is therefore called thymus-independent antigens or T cell-independent antigens (TI-Ag) (*8, 31*). In contrast, T-dependent antigens (TD-Ag) mainly include proteins/peptides that are uptaken by the antigen-presenting cells and presented in the context with major histo-compatibility complex type 2 (MHC II) to the T helper lymphocytes (*8, 31*). According to its chemical nature, PEGylated LNP is similar to PEGylated liposome and belongs to TI-Ag, as it doesn’t contain any proteinatious composition. Traditionally, there has been a perception that TI-Ag could not induce isotype switch from IgM to long-lasting IgG, resulting in the production of IgM only (no or very low level of IgG) after administration of TI-Ag. Moreover, it is generally believed that TI-Ag is not able to induce a typical recall antibody response, which is also called immunological memory or B cell memory characterized by an amplified, accelerated and affinity-matured antibody production after successive exposure to certain antigens such as TD-Ag (*35-36*). Consistent with these theories, even six repeated injections of PEGylated liposome (with a seven-day interval) did not enhance the anti-PEG IgM production in mice, and the anti-PEG IgG level remained extremely low throughout the study (*37*). Interestingly, after a thorough literature search, we found that although three types of TI-Ag, including B. hermsii (Borrelia hermsii, a relapsing fever bacterium), NP-Ficoll (4-hydroxy-3-nitrophenylacetyl-Ficoll, a model TI-Ag) and pneumococcal capsular PS3 (serotype 3 capsular polysaccharide), could induce immune memory (*38-40*), previously there is no report on either inducing immune memory or isotype switching from IgM to IgG by any PEG derivatives belonging to TI-Ag. Herein, unexpectedly we discovered that different from other PEG derivatives which belong to TI-Ag such as PEGylated liposome, PEGylated LNP could not only induce isotype switch and subsequent production of anti-PEG IgG (Fig. 4, A and C), but cause immune memory/B cell memory, leading to rapid enhancement and longer lasting time of both anti-PEG IgM and IgG upon repeated injection (Fig. 5, Table 3 and Table 4). These findings will refresh our understandings and break our traditional expectations on PEGylated LNP, and possible other PEG derivatives belonging to TI-Ag.

Materials and Methods

Materials

Cholesterol and DSPC were purchased from Lipoid GMBH (Ludwigshafen, Germany).

ALC-0315 and ALC-0159 were acquired from SINOPEG (Xiamen, China). Ferric chloride hexahydrate, ammonium thiocyanate and polyethylene glycols (PEG_{10000}) were obtained from Sigma-Aldrich (St. Louis, MO, USA). 3-[(3-cholamidopropyl)dimethylammonio]-1-propanesulfonate (CHAPS), 3,3′,5,5′-Tetramethylbenzidine dihydrochloride hydrate (TMB 2HCl) and nonfat powdered milk were purchased from Beyotime Biotechnology (Shanghai, China). Maxisorp 96-well microplates were acquired from Nalge-Nunc International (Rochester, NY, USA). D-Luciferin were purchased from Thermo Fisher Scientific (Waltham, MA, USA). Firefly luciferase mRNA was obtained from Trilink Biotechnologies (San Diego, CA, USA). Rat anti-PEG IgM (rAGP6-PABM-A) and rat anti-PEG IgG (r33G-PABG-A) were acquired from Academia Sinica (Taipei, China). Peroxidase-conjugated affinipure rabbit anti-rat IgM μ-chain specific and peroxidase-conjugated affinipure donkey anti-rat IgG (H+L) were obtained from Jackson ImmunoResearch Laboratories Inc (West Grove, PA, USA).

Preparation of LNP, DiR-LNP and DiR-LU@LNP

LNP, DiR-LNP and DiR-LU@LNP were formulated according to a previously reported protocol (*27*). First, the ethanol phase was prepared by dissolving ALC-0315, DSPC, cholesterol and ALC-0159 at a molar ratio of 46.3: 9.4: 42.7: 1.6. Specifically, DiR was added into the ethanol phase at 0.4% mol for preparation of DiR-LNP and DiR-LU@LNP. Regarding the aqueous phase, it was prepared using 20 mM citrate buffer (pH4.0) for LNP and DiR-LNP formulations, with additional firefly luciferase mRNA added for DiR-LU@LNP formulation. Subsequently, the ethanol phase was mixed with the aqueous phase at a flow rate ratio of 1: 3 (ethanol: aqueous) through a microfluidic mixer (Precision Nanosystems Inc., Canada). Afterwards, the obtained nanoparticle solutions were dialyzed against 10×volume of PBS (pH7.4) through a tangential-flow filtration (TFF) membrane with 100 kD molecular weight cut-off (Sartorius Stedim Biotech, Germany) for at least 18 hours. Finally, nanoparticle solutions were concentrated using Amicon ultra-centrifugal filters (EMD Millipore, Billerica, MA, USA), passed through a 0.22 μm filter and stored at 2~8□ until use.

Characterization of LNP, DiR-LNP and DiR-LU@LNP

LNP, DiR-LNP and DiR-LU@LNP were examined for their hydrodynamic size (Z-average), polydispersity index (PDI) and zeta potential with DLS (Zetasizer Nano ZS, Malvern Instruments Ltd, Malvern, UK) equipped with a solid state HeNe laser (λ=633 nm) at a scattering angle of 173˚. Nanoparticles were either added into PBS (pH7.4) for Z-average and PDI measurements, or added into ultrapure water for determination of zeta potential. Three independent experiments were conducted, with each type of LNP examined at 25˚C for 10 seconds (pre-equilibration for 2 minutes) and repeated at least 10 times in disposable cuvettes (for Z-average and PDI) or zeta cuvettes (for zeta potential). The obtained data were presented as “mean ± standard deviation”. To further assess their stability in serum (simulating in vivo environment in this study), LNP, DiR-LNP and DiR-LU@LNP were diluted to 1:100 with PBS containing 10% rat serum and then

incubated at 37□ for 24 hours. Subsequently, 1 mL of diluted LNP, DiR-LNP and DiR-LU@LNP were respectively collected at designated time points (1 hour, 6 hours, 12 hours and 24 hours post-incubation), followed by characterization of Z-average and PDI with DLS. Three independent experiments were conducted, with each type of LNP examined at 37˚C for 10 seconds (pre-equilibration for 2 minutes) and repeated at least 10 times in disposable cuvettes. The obtained data were presented as "mean ± standard deviation". Furthermore, the morphological characteristics of LNP, DiR-LNP and DiR-LU@LNP were observed with Cryo-TEM. In brief, 3 μL of each LNP sample was deposited onto a holey carbon grid that was glow-discharged (Quantifoil R1.2/1.3) and vitrificated using a Vitrobot Mark IV System (FEI/Thermo Scientific, Waltham, MA, USA). Cryo-TEM imaging was performed on a Talos F200C device (FEI/Thermo Scientific, Waltham, MA, USA) equipped with a 4k × 4k Ceta camera at 200 kV accelerating voltage in the Center of Cryo-Electron Microscopy, Zhejiang University.

In addition, the phospholipid (DSPC) concentrations of LNP, DiR-LNP and DiR-LU@LNP solutions were quantified via Steward's assay for further calculation of LNP doses (*42*). Briefly, ammonium ferrothiocynate was prepared by dissolving 27.03 mg ferric chloride hexahydrate and 30.4 mg ammonium thiocyanate in 1 mL of distilled water. 10 μL of the lipid sample was added to 990 μL of chloroform, followed by addition of 1 mL of ammonium ferrothiocynate. The obtained mixture was vortexed for 60 seconds and then centrifuged at 1000 rpm for 15 minutes at room temperature. The bottom chloroform layer was transferred to a glass cuvette and the absorbance was measured at 470 nm using a Unicam UV500 Spectrophotometer (Thermo electron corporation, USA). Standard curves for DSPC lipid were obtained and used for calculation of the phospholipid concentrations of LNP, DiR-LNP and DiR-LU@LNP solutions. Eventually, the various doses of LNP tested in the animal experiments were calculated based on the phospholipid (DSPC) exposure amount per dose of related drug (see below for details).

Determination of LNP dosing protocols

1) Calculation of $mPEG_{2000}$ and phospholipid (DSPC) exposure amount of three FDA-approved LNP-delivered therapeutics (using 60 kg as the reference body weight of an adult)

I. BNT162b2: According to its published formulation and clinical protocols (*21*), the $mPEG_{2000}$ contained in each dose of BNT162b2 in adults is approximately 0.0406 mg. Correspondingly, the exposure amount of phospholipid (DSPC) is 0.09 mg per dose of this mRNA vaccine.

II. mRNA-1273: According to its published formulation and clinical protocols (*22*), the maximum exposure amount of $mPEG_{2000}$ is 1.5385 mg per dose of mRNA-1273 in adults, which is around 38 times that of BNT162b2.

III. Patisiran: According to its published formulation and clinical protocols (*20*), the $mPEG_{2000}$ exposure amount is approximately 10.6434 mg per injection of Patisiran in adults, which is 262 times that of BNT162b2.

2) Conversion of human dosage to equivalent dosage in rat and determination of three

clinically relevant LNP doses

According to the animal-human dose exchange algorithm: animal equivalent dose=human dose × K_m ratio (6.2 for rat) (*43*), three clinically relevant LNP doses for rats were as follows: low dose (L-LNP), 0.009 mg phospolipid/kg (0.09 mg/60 kg × 6.2), related with $mPEG_{2000}$ exposure amount in each BNT162b2 injection; middle dose (M-LNP), 0.342 mg phospholipids/kg (0.009 × 38), related with $mPEG_{2000}$ exposure amount in each mRNA-1273 injection; high dose (H-LNP), 2.358 mg phospholipids/kg (0.009 × 262), related with $mPEG_{2000}$ exposure amount in each Patisiran injection.

3) Determination of LNP administration route, frequency and interval

The clinical protocols of BNT162b2 were essentially simulated in this study. That is, LNP was administrated through intramuscular injection for two separate injections, with a 21-day interval (same as routine vaccination).

Animals

10-12-week-old female Wistar rats were purchased from Hangzhou Medical College (Hangzhou, China), and maintained in the Laboratory Animal Center of Zhejiang University under controlled environmental conditions at constant temperature, humidity, and a 12-hour dark/light cycle. Rats were given ad libitum access to a standard rat chow and water, and were acclimated for at least 7 days. All animal experiments were approved by the Laboratory Animal Welfare and Ethnics Committee of Zhejiang University and carried out in accordance with the guidelines of the committee (approval No. ZJU20210071).

Administration of LNP simulating clinical protocols and collection of serum samples for ELISA

Wistar rats were randomly divided into a Control group (n=8) and three LNP-treated groups (n=15). At Day 0, LNP-treated groups were intramuscularly injected with 0.009 mg phospholipids/kg LNP (L-LNP group), 0.342 mg phospholipids/kg LNP (M-LNP group) and 2.358 mg phospholipids/kg LNP (H-LNP group), respectively, while the Control group only received PBS. At Day 21, rats in each experimental group received same treatment as the initial injection. Peripheral blood samples of each rat were collected successively via the retro-orbital venous plexus at Day 0, 3, 5, 7, 14, 21, 24, 26, 28, 35, 42 and 49. All blood samples were centrifuged at 2000 × g for 15 minutes at 4 °C, and the serums were immediately stored at -80 °C for further quantification of anti-PEG antibody.

Quantification of anti-PEG IgM and anti-PEG IgG antibodies with ELISA

Maxisorp 96-well microplates were coated with 5 μg/well PEG_{10000} in 100 μL of PBS overnight at 4 □. Subsequently, plates were gently washed with 350 μL of washing buffer (0.05% (w/v) CHAPS in DPBS) for three times, followed by incubation with blocking buffer (5% (w/v) skim milk powder in DPBS, 200 μL/well) at room temperature for 1.5 hours. Afterwards, plates

were washed with washing buffer for three times again. Then 100 μL of rat serum samples diluted 1: 150 with dilution buffer (2% (w/v) skim milk powder in DPBS), together with serial dilutions of rat anti-PEG IgM and rat anti-PEG IgG standards, were added into anti-PEG IgM and anti-PEG IgG detection plates in duplicate and further incubated for 1 hour at room temperature. After five successive washes, 50 μL of diluted peroxidase-conjugated affinipure rabbit anti-rat IgM μ-chain specific and peroxidase-conjugated affinipure donkey anti-rat IgG (H+L) antibodies were respectively added to the corresponding plates and incubated for 1 hour at room temperature. Again, unbounded antibodies were removed by five washes, followed by incubation with 100 μL of TMB for 30 minutes at room temperature. Finally, HRP-TMB reaction was stopped with 100 μL of 2 N H_2SO_4, and the absorbance was measured at 450 nm with a microplate reader (Thermo Fisher Scientific, Waltham, MA, USA), using 570 nm as a reference wavelength. Anti-PEG IgM and anti-PEG IgG standard curves were constructed by plotting the average corrected absorbance values ($OD_{450\ nm}$-$OD_{570\ nm}$) and corresponding antibody concentrations with Origin 2021 software. Concentrations of anti-PEG IgG and IgM antibodies in serum samples were calculated based on the standard curves. In addition, assay precision was determined by calculating the mean Coefficient of Variation (CV%=(Standard deviation/Mean) × 100%) for all detectable standards and samples in all batches of ELISA.

Biodistribution of PEGylated LNP in major organs of Wistar rats

Wistar rats were randomly divided into a Control group and three DiR-LU@LNP-treated groups (n=6). At Day 0, LNP-treated groups were intramuscularly injected with 0.009 mg phospholipids/kg DiR-LU@LNP (L-LNP group), 0.342 mg phospholipids/kg DiR-LU@LNP (M-LNP group) and 2.358 mg phospholipids/kg DiR-LU@LNP (H-LNP group), respectively, while the Control group only received PBS. At Day 21, rats in each experimental group received same treatment as the initial injection. Six hours after the first and second injections, three rats in each group were administered intraperitoneally with D-luciferin at a dose of 150 mg/kg. Rats were sacrificed 15 minutes after D-luciferin administration and immediately dissected for collection of several primary organs, including heart, liver, spleen, lung, kidneys, draining lymph node and muscle at the injection site. Whole-organ/tissue imaginings for DiR fluorescence (Excitation/Emission: 748 nm/780 nm) and firefly luciferase bioluminescence were performed with IVIS Spectrum imaging system and analyzed with Living Image software (Caliper Life Sciences, Waltham, Massachusetts, USA). Meanwhile, all organs or tissues were weighed for normalization of the total organ/tissue fluorescence by the organ mass.

Blood clearance of PEGylated LNP in Wistar rats

Wistar rats were randomly divided into a Control group and three DiR-LNP-treated groups (n=3). At Day 0, LNP-treated groups were intramuscularly injected with 0.009 mg phospholipids/kg DiR-LNP (L-LNP group), 0.342 mg phospholipids/kg DiR-LNP (M-LNP group) and 2.358 mg phospholipids/kg DiR- LNP (H-LNP group), respectively, while the Control group

only received PBS. At Day 21, rats in each experimental group received same treatment as the initial injection. Peripheral blood samples were respectively collected from the retro-orbital venous plexus at 5 minutes, 30 minutes, 1 hour, 3 hours, 6 hours, 10 hours, 24 hours and 48 hours after the first and second injections. Then blood samples were centrifuged at 2000×g at 4 °C for 15 minutes, and serum samples were isolated and immediately stored in dark at -80 °C. DiR fluorescence associated with LNP in serum samples was detected by fluorescent spectroscopy on a Spectramax ID5 (Molecular Devices, San Jose, California, USA) at excitation/emission wavelengths of 748/780 nm.

Data presentation and statistical analysis

All data were presented as "mean ± standard deviation". Concentrations of anti-PEG IgM and anti-PEG IgG were analyzed after $\log_{10}$ transformation, and their differences among various groups at each time point were analyzed with Mann-Whitney U test using R 4.0.5 (R Software, Boston, MA, USA), with *P* values adjusted for FDR (false discovery rate). Changing curves of average level of anti-PEG antibody over time for various doses were fitted by the R package called "ggalt". Profile analysis was performed to examine whether the overall trends of changing curves of average level of anti-PEG antibody over time between every two groups were equal. The analysis included two parts: parallel test and coincidence test. Only when the two changing curves of average level of anti-PEG antibody met both parallel and coincidence test, the overall trend of the two changing curves of average level of anti-PEG antibody was considered to be no difference. According to factorial design (group × time) and repeated measures of antibody level, linear mixed models (LMM) were conducted to compare the change rates and average levels of anti-PEG antibody across groups, with all time points included. Several variables, including group (indicating mean differences in the average levels of anti-PEG antibody), time, time^2, number of injections, and interaction term of group and time (indicating mean differences in the change rates of anti-PEG antibody) as fixed effect and subject as random effect were considered in LMM.

In addition, ▲Anti-PEG IgM (Log_{10} CONC) was defined as Anti-PEG IgM (Log_{10} $\text{CONC}_{2\text{nd injection}}$) ($\log_{10}$-transformed concentration of anti-PEG IgM induced during the second injection cycle) subtracting corresponding Anti-PEG IgM (Log_{10} $\text{CONC}_{1\text{st injection}}$) ($\log_{10}$-transformed concentrations of anti-PEG IgM induced during the first injection cycle). Similarly, ▲Anti-PEG IgG (Log_{10} CONC) was calculated by subtracting Anti-PEG IgG (Log_{10} $\text{CONC}_{1\text{st injection}}$) ($\log_{10}$-transformed concentrations of anti-PEG IgG induced during the first injection cycle) from the corresponding Anti-PEG IgG (Log_{10} $\text{CONC}_{2\text{nd injection}}$) ($\log_{10}$-transformed concentration of anti-PEG IgG induced during the second injection cycle). Differences in ▲Anti-PEG IgM (Log_{10} CONC) or ▲Anti-PEG IgG (Log_{10} CONC) among various groups at each time point were analyzed with Mann-Whitney U test using R 4.0.5, with *P* values adjusted for FDR (false discovery rate). Changing curves of average level of ▲Anti-PEG IgM (Log_{10} CONC) or ▲Anti-PEG IgG (Log_{10} CONC) over time for various doses were fitted by the R package called "ggalt". Profile analysis was performed to examine whether the overall trends of changing curves of

average level of ▲Anti-PEG IgM (Log_{10} CONC) or ▲Anti-PEG IgG (Log_{10} CONC) over time between every two groups were equal. The analysis included two parts: parallel test and coincidence test. Only when the two changing curves of average level of ▲Anti-PEG IgM (Log_{10} CONC) or ▲Anti-PEG IgG (Log_{10} CONC) met both parallel and coincidence test, the overall trend of the two changing curves of average level of ▲Anti-PEG IgM (Log_{10} CONC) or ▲Anti-PEG IgG (Log_{10} CONC) was considered to be no difference. According to factorial design (group × time) and repeated measures of antibody level, LMM were conducted to compare the change rates and average levels of ▲Anti-PEG IgM (Log_{10} CONC) or ▲Anti-PEG IgG (Log_{10} CONC) across groups, with all time points included. Several variables, including group (indicating mean differences in the average levels of ▲Anti-PEG IgM (Log_{10} CONC) or ▲Anti-PEG IgG (Log_{10} CONC)), time, $time^2$, and interaction term of group and time (indicating mean differences in the change rates of ▲Anti-PEG IgM (Log_{10} CONC) or ▲Anti-PEG IgG (Log_{10} CONC) levels) as fixed effect and subject as random effect were considered in LMM. Data obtained in the biodistribution and blood clearance study were analyzed using multiple unpaired *t* tests with correction for multiple comparisons using Prism 9.2.0 (GraphPad Software, San Diego, USA). $P<0.05$ was considered statistically significant.

References

1. J.A. Kulkarni, D. Witzigmann, S.B. Thomson, S. Chen, B.R. Leavitt, P.R. Cullis, R. van der Meel, The current landscape of nucleic acid therapeutics. Nat. Nanotechnol. **16**, 630-643 (2021).
2. J. Szebeni, G. Storm, J.Y. Ljubimova, M. Castells, E.J. Phillips, K. Turjeman, Y. Barenholz, D.J.A. Crommelin, M.A. Dobrovolskaia, Applying lessons learned from nanomedicines to understand rare hypersensitivity reactions to mRNA-based SARS-CoV-2 vaccines. Nat. Nanotechnol. **17**, 337-346 (2022).
3. B.B. Mendes, J. Conniot, A. Avital, D. Yao, X. Jiang, X. Zhou, N. Sharf-Pauker, Y. Xiao, O. Adir, H. Liang, J. Shi, A. Schroeder, J. Conde, Nanodelivery of nucleic acids. Nat Rev Methods Primers **2**, (2022).
4. A. Curreri, D. Sankholkar, S. Mitragotri, Z. Zhao, RNA therapeutics in the clinic. Bioeng. Transl. Med., (2022).
5. J. S. Suk, Q. G. Xu, N. Kim, J. Hanes, L. M. Ensign, PEGylation as a strategy for improving nanoparticle-based drug and gene delivery. Adv. Drug. Deliver. Rev. **99**, 28-51 (2016).
6. A. Khurana, P. Allawadhi, I. Khurana, S. Allwadhi, R. Weiskirchen, A.K. Banothu, D. Chhabra, K. Joshi, K.K. Bharani, Role of nanotechnology behind the success of mRNA vaccines for COVID-19. Nano Today **38**, (2021).
7. A. W. Richter, E. Akerblom, Antibodies against polyethylene-glycol produced in animals by immunization with monomethoxy polyethylene-glycol modified proteins. Int. Arch. Aller. Imm. **70**, 124-131 (1983).
8. B. M. Chen, T. L. Cheng, S. R. Roffler, Polyethylene glycol immunogenicity: Theoretical, clinical, and practical aspects of anti-polyethylene glycol antibodies. Acs Nano **15**, 14022-14048 (2021).
9. H. F. Haddad, J. A. Burke, E. A. Scott, G. A. Ameer, Clinical Relevance of pre-existing and treatment-induced anti-poly(ethylene glycol) antibodies. Regen. Eng. Transl. Med. **8**, 32-42 (2022).
10. T.T.H. Thi, E.H. Pilkington, D.H. Nguyen, J.S. Lee, K.D. Park, N.P. Truong, The importance of poly(ethylene glycol) alternatives for overcoming PEG immunogenicity in drug delivery

and bioconjugation. Polymers-Basel **12**, (2020).
11. A. S. Abu Lila, H. Kiwada, T. Ishida, The accelerated blood clearance (ABC) phenomenon: clinical challenge and approaches to manage. J. Control. Release **172**, 38-47 (2013).
12. T. L. Cheng, P. Y. Wu, M. F. Wu, J. W. Chern, S. R. Roffler, Accelerated clearance of polyethylene glycol-modified proteins by anti-polyethylene glycol IgM. Bioconjug. Chem. **10**, 520-528 (1999).
13. T. Ishida, M. Ichihara, X. Wang, K. Yamamoto, J. Kimura, E. Majima, H. Kiwada, Injection of PEGylated liposomes in rats elicits PEG-specific IgM, which is responsible for rapid elimination of a second dose of PEGylated liposomes. J. Control. Release **112**, 15-25 (2006).
14. J.K. Armstrong, G. Hempel, S. Koling, L.S. Chan, T. Fisher, H.J. Meiselman, G. Garratty, Antibody against poly(ethylene glycol) adversely affects PEG-asparaginase therapy in acute lymphoblastic leukemia patients. Cancer **110**, 103-111 (2007).
15. M.S. Hershfield, N.J. Ganson, S.J. Kelly, E.L. Scarlett, D.A. Jaggers, J.S. Sundy, Induced and pre-existing anti-polyethylene glycol antibody in a trial of every 3-week dosing of pegloticase for refractory gout, including in organ transplant recipients. Arthritis Res. Ther. **16**, R63 (2014).
16. X.P. Zhang, V. Goel, H. Attarwala, M.T. Sweetser, V.A. Clausen, G.J. Robbie, Patisiran pharmacokinetics, pharmacodynamics, and exposure-response analyses in the phase 3 APOLLO trial in patients with hereditary transthyretin-mediated (hATTR) amyloidosis. J. Clin. Pharmacol. **60**, 37-49 (2020).
17. Y. Ju, W.S. Lee, E.H. Pilkington, H.G. Kelly, S. Li, K.J. Selva, K.M. Wragg, K. Subbarao, T.H.O. Nguyen, L.C. Rowntree, L.F. Allen, K. Bond, D.A. Williamson, N.P. Truong, M. Plebanski, K. Kedzierska, S. Mahanty, A.W. Chung, F. Caruso, A.K. Wheatley, J.A. Juno, S.J. Kent, Anti-PEG antibodies boosted in humans by SARS-CoV-2 lipid nanoparticle mRNA vaccine. Acs Nano **16**, 11769–11780 (2022).
18. G. Guerrini, S. Gioria, A.V. Sauer, S. Lucchesi, F. Montagnani, G. Pastore, A. Ciabattini, D. Medaglini, L. Calzolai, Monitoring anti-PEG antibodies level upon repeated lipid nanoparticle-based COVID-19 vaccine administration. Int. J. Mol. Sci. **23**, (2022).
19. J.M. Carreno, G. Singh, J. Tcheou, K. Srivastava, C. Gleason, H. Muramatsu, P. Desai, J.A. Aberg, R.L. Miller, P. Study Group, N. Pardi, V. Simon, F. Krammer, mRNA-1273 but not BNT162b2 induces antibodies against polyethylene glycol (PEG) contained in mRNA-based vaccine formulations. Vaccine **40**, 6114-6124 (2022).
20. Food and Drug Administration. ONPATTRO (patisiran) lipid complex injection addendum to drug product quality review, 14 February, 2017; https://www.accessdata.fda.gov/drugsatfda_docs/nda/2018/210922Orig1s000ChemR.pdf.
21. Food and Drug Administration. Comirnaty Information-Summary basis for regulatory action, 8 November, 2021; https://www.fda.gov/media/151733/download
22. Food and Drug Administration. Spikevax Information-Summary basis for regulatory action, 30 January, 2022; https://www.fda.gov/media/155931/download
23. M. Danaei, M. Dehghankhold, S. Ataei, F.H. Davarani, R. Javanmard, A. Dokhani, S. Khorasani, M.R. Mozafari, Impact of particle size and polydispersity index on the clinical applications of lipidic nanocarrier systems. Pharmaceutics **10**, 57 (2018).
24. Y. Eygeris, M. Gupta, J. Kim, G. Sahay, Chemistry of lipid nanoparticles for RNA delivery. Acc. Chem. Res. **55**, 2-12 (2022).
25. K. Yang, C. Reker-Smit, M. C. A. Stuart, A. Salvati, Effects of protein source on liposome uptake by cells: Corona composition and impact of the excess free proteins. Adv. Healthc. Mater. **10**, e2100370 (2021).
26. V.A. Naumenko, S.S. Vodopyanov, K.Y. Vlasova, D.M. Potashnikova, P.A. Melnikov, D.A. Vishnevskiy, A.S. Garanina, M.P. Valikhov, A.V. Lipatova, V.P. Chekhonin, A.G. Majouga, M.A. Abakumov, Intravital imaging of liposome behavior upon repeated administration: A

step towards the development of liposomal companion diagnostic for cancer nanotherapy. J. Control. Release **330**, 244-256 (2021).

27. M. Ibrahim, E. Ramadan, N.E. Elsadek, S.E. Emam, T. Shimizu, H. Ando, Y. Ishima, O.H. Elgarhy, H.A. Sarhan, A.K. Hussein, T. Ishida, Polyethylene glycol (PEG): The nature, immunogenicity, and role in the hypersensitivity of PEGylated products. J. Control. Release **351**, 215-230 (2022).
28. Q. Yang, S.K. Lai, Anti-PEG immunity: emergence, characteristics, and unaddressed questions. Wiley Interdiscip. Rev. Nanomed. Nanobiotechnol. **7**, 655-677 (2015).
29. B.M. Chen, Y.C. Su, C.J. Chang, P.A. Burnouf, K.H. Chuang, C.H. Chen, T.L. Cheng, Y.T. Chen, J.Y. Wu, S.R. Roffler, Measurement of pre-existing IgG and IgM antibodies against polyethylene glycol in healthy individuals. Anal. Chem. **88**, 10661-10666 (2016).
30. Q. Yang, T.M. Jacobs, J.D. McCallen, D.T. Moore, J.T. Huckaby, J.N. Edelstein, S.K. Lai, Analysis of Pre-existing IgG and IgM antibodies against polyethylene glycol (PEG) in the general population. Anal. Chem. **88**, 11804-11812 (2016).
31. D. Shi, D. Beasock, A. Fessler, J. Szebeni, J.Y. Ljubimova, K.A. Afonin, M.A. Dobrovolskaia, To PEGylate or not to PEGylate: Immunological properties of nanomedicine's most popular component, polyethylene glycol and its alternatives. Adv. Drug Deliver. Rev. **180**, 114079 (2022)
32. World Health Organization. WHO guidelines on non-clinical evaluation of vaccines, WHO Technical Report Series No. 927, Annex 1, 1 January 2005; https://cdn.who.int/media/docs/default-source/biologicals/vaccine-standardization/annex-1nonclinical.p31-63.pdf?sfvrsn=e87c28d8_3&download=true
33. European Medicines Agency. Spikevax (previously COVID-19 Vaccine Moderna) : EPAR - Public assessment report, 20 January 2021; https://www.ema.europa.eu/en/documents/assessment-report/spikevax-previously-covid-19-vaccine-moderna-epar-public-assessment-report_en.pdf
34. European Medicines Agency. Comirnaty : EPAR - Public assessment report, 23 December 2020; https://www.ema.europa.eu/en/documents/assessment-report/comirnaty-epar-public-assessment-report_en.pdf
35. G.T. Kozma, T. Shimizu, T. Ishida, J. Szebeni, Anti-PEG antibodies: Properties, formation, testing and role in adverse immune reactions to PEGylated nano-biopharmaceuticals. Adv. Drug Deliver. Rev.**154**, 163-175 (2020).
36. T. Defrance, M. Taillardet, L. Genestier, T cell-independent B cell memory. Curr. Opin. Immunol. **23**, 330-336 (2011).
37. M. Ichihara, T. Shimizu, A. Imoto, Y. Hashiguchi, Y. Uehara, T. Ishida, H. Kiwada, Anti-PEG IgM response against PEGylated liposomes in mice and rats. Pharmaceutics **3**, 1-11 (2010).
38. K.R. Alugupalli, J.M. Leong, R.T. Woodland, M. Muramatsu, T. Honjo, R.M. Gerstein, B1b lymphocytes confer T cell-independent long-lasting immunity. Immunity **21**, 379-390 (2004).
39. T.V. Obukhanych, M.C. Nussenzweig, T-independent type II immune responses generate memory B cells. J. Exp. Med. **203**, 305-310 (2006).
40. M. Taillardet, G. Haffar, P. Mondiere, M.J. Asensio, H. Gheit, N. Burdin, T. Defrance, L. Genestier, The thymus-independent immunity conferred by a pneumococcal polysaccharide is mediated by long-lived plasma cells. Blood **114**, 4432-4440 (2009).
41. N.N. Zhang, X.F. Li, Y.Q. Deng, H. Zhao, Y.J. Huang, G. Yang, W.J. Huang, P. Gao, C. Zhou, R.R. Zhang, Y. Guo, S.H. Sun, H. Fan, S.L. Zu, Q. Chen, Q. He, T.S. Cao, X.Y. Huang, H.Y. Qiu, J.H. Nie, Y.H. Jiang, H.Y. Yan, Q. Ye, X. Zhong, X.L. Xue, Z.Y. Zha, D.S. Zhou, X. Yang, Y.C. Wang, B. Ying, C.F. Qin, A thermostable mRNA vaccine against COVID-19. Cell **182**, 1271-1283 (2020).
42. J. C. M. Stewart, Colorimetric Determination of phospholipids with ammonium ferrothiocyanate. Anal. Biochem. **104**, 10-14 (1980).

43. A. Nair, M.A. Morsy, S. Jacob, Dose translation between laboratory animals and human in preclinical and clinical phases of drug development. Drug. Dev. Res. **79**, 373-382 (2018)

Figures and Tables

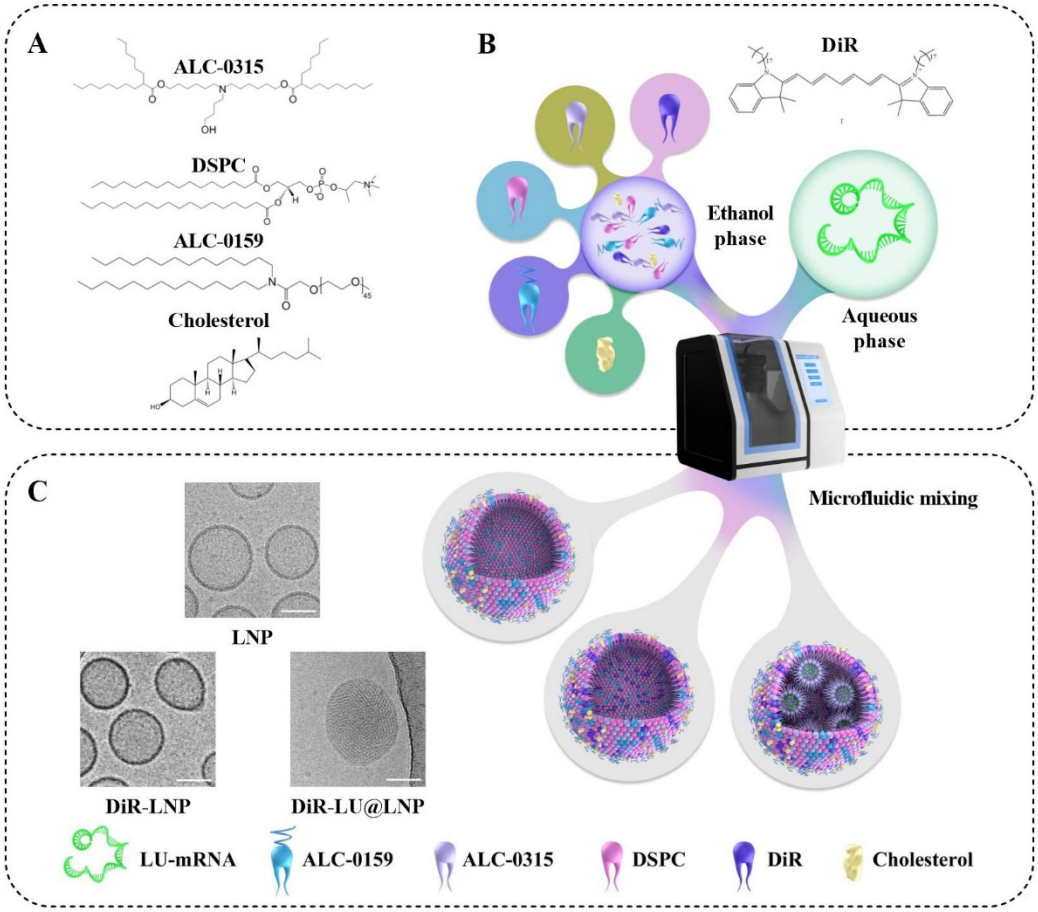

Fig. 1. Preparation of LNP, DiR-LNP and DiR-LU@LNP. (**A**) Chemical structures of lipid compositions in LNP carrier of COVID-19 vaccine BNT162b2. (**B**) Schematic illustration of the synthesis of LNP, DiR-LNP and DiR-LU@LNP. Briefly, the ethanol phase was combined with the aqueous phase at a flow rate ratio of 1: 3 (ethanol: aqueous) through a microfluidic mixing device. (**C**) Representative cryogenic transmission electron microscopy (Cryo-TEM) images of LNP, DiR-LNP and DiR-LU@LNP. Scale bar: 50 nm. LNP, lipid nanoparticles; LU-mRNA: luciferase mRNA.

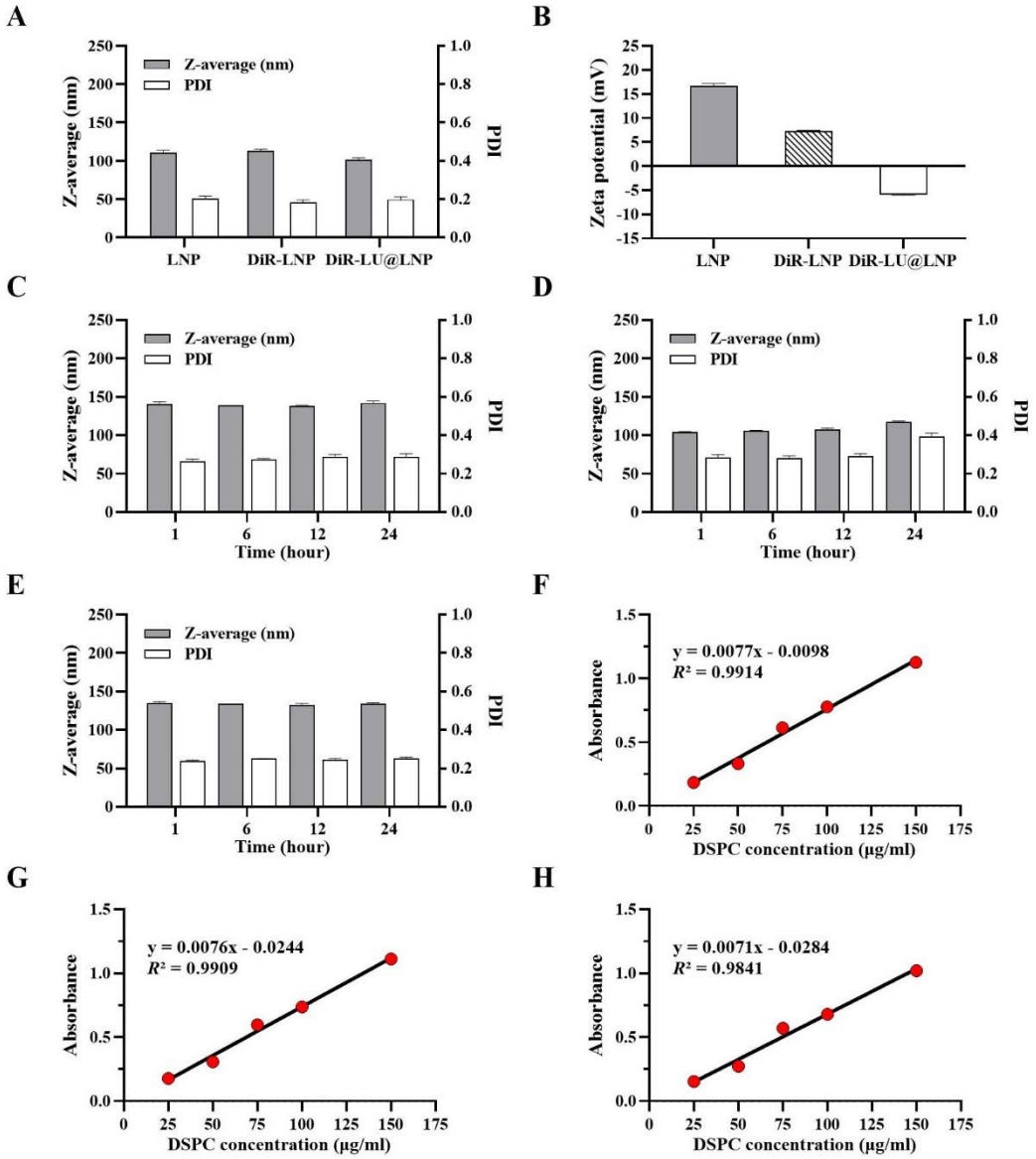

Fig. 2. Characterization of LNP, DiR-LNP and DiR-LU@LNP. (**A**) Hydrodynamic size (Z-average) and polydispersity index (PDI) of LNP, DiR-LNP and DiR-LU@LNP measured by DLS. (**B**) Zeta potential of LNP, DiR-LNP and DiR-LU@LNP measured by DLS. (**C-E**) Stability of (C) LNP, (D) DiR-LNP and (E) DiR-LU@LNP in serum. LNP, DiR-LNP and DiR-LU@LNP were diluted to 1:100 with PBS containing 10% rat serum and incubated at 37□ for 24 hours. Subsequently, 1 mL of diluted LNP, DiR-LNP and DiR-LU@LNP were respectively collected at designated time points (1 hour, 6 hours, 12 hours and 24 hours), followed by characterization of Z-average and PDI with dynamic light scattering. (**F-H**) Standard curves for determining phospholipid (DSPC) concentration in (F) LNP, (G) DiR-LNP and (H) DiR-LU@LNP solutions. Data were presented as “mean ± standard deviation” of three independent experiments.

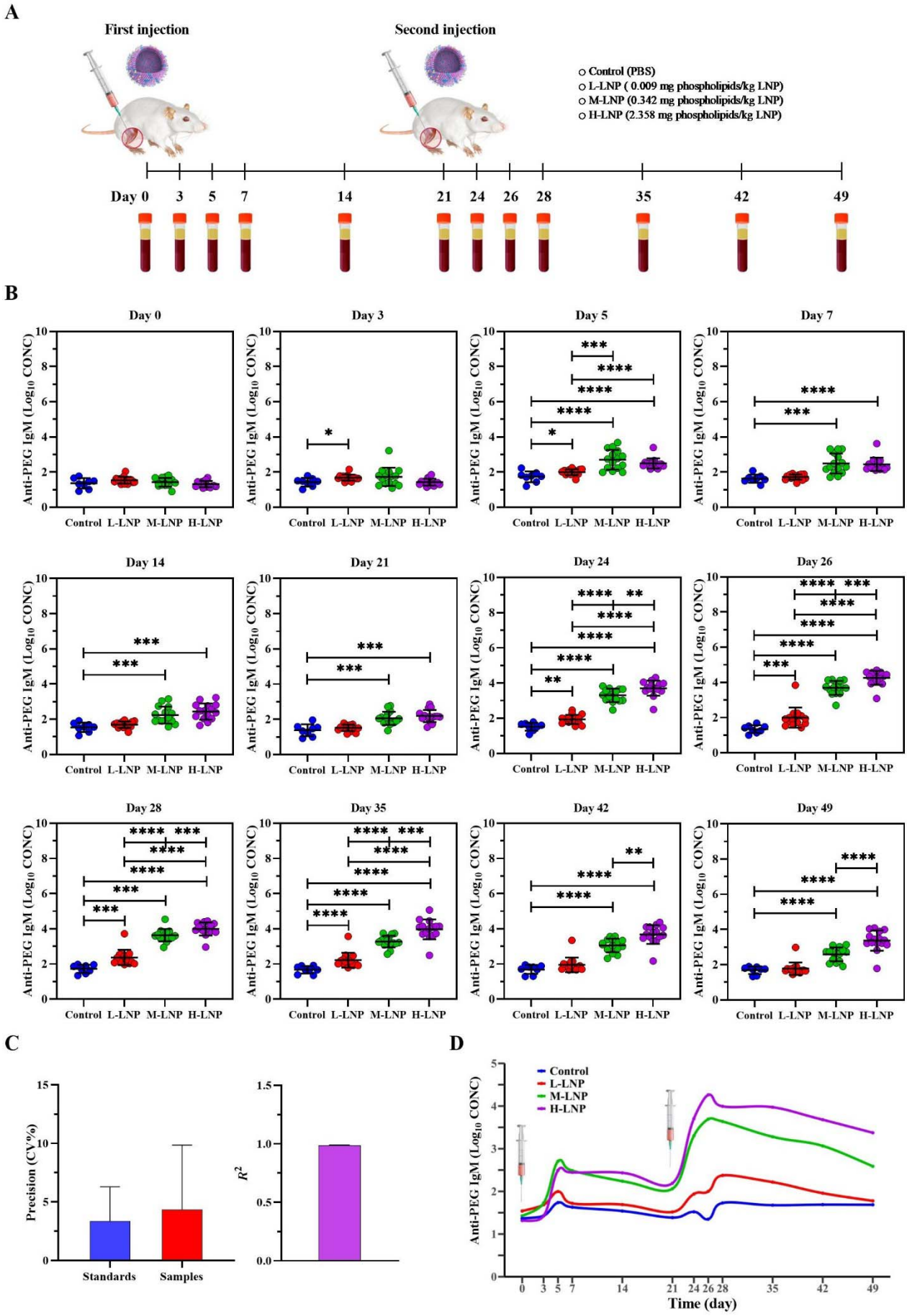
A
First injection
Second injection
Control (PBS)
L-LNP (0.009 mg phospholipids/kg LNP)
M-LNP (0.342 mg phospholipids/kg LNP)
H-LNP (2.358 mg phospholipids/kg LNP)
Day 0
3
5
7
14
21
24
26
28
35
42
49
B
Day 0
Day 3
Day 5
Day 7
Day 14
Day 21
Day 24
Day 26
Day 28
Day 35
Day 42
Day 49
Anti-PEG IgM (Log10 CONC)
Control
L-LNP
M-LNP
H-LNP
C
Precision (CV%)
Standards
Samples
R2
D
Control
L-LNP
M-LNP
H-LNP
Anti-PEG IgM (Log10 CONC)
Time (day)

Fig. 3. Experimental design and evaluation of anti-PEG IgM production in rat. (**A**) Schematic illustration of the experimental protocols. Wistar rats were injected intramuscularly with 0.009 (L-LNP group), 0.342 (M-LNP group) or 2.358 (H-LNP) mg phospholipids/kg LNP on Day 0 and Day 21, respectively. Rats in the Control group were injected with PBS. Serum samples were collected at the indicated time points (Day 0, 3, 5, 7, 14, 21, 24, 26, 28, 35, 42 and 49) for further evaluation of the presence and level of anti-PEG antibodies with ELISA. (**B**) Quantitative analysis of anti-PEG IgM (Log_{10} CONC) (log_{10}-transformed concentration of anti-PEG IgM) induced by LNP in rat serum. Data were presented as "mean ± standard deviation", with n=8 for Control group and n=15 for all LNP-treated groups. Differences in anti-PEG IgM (Log_{10} CONC) among various groups were analyzed using Mann-Whitney U test, with *P* values adjusted for FDR (false discovery rate). *, $P<0.05$; **, $P<0.01$; ***, $P<0.001$; ****, $P<0.0001$. (**C**) Excellent quality control of ELISA for determination of anti-PEG IgM. The left image shows the average precision/CV (coefficient of variation) of standards and samples in ELISA, and the right image shows the mean linear regression coefficient of determination of the standard curve for ELISA. (**D**) Time-course of anti-PEG IgM induced by PEGylated LNP. The changing curves of mean anti-PEG IgM (Log_{10} CONC) levels over time were fitted by the R package called "ggalt".

Table 1. Linear mixed model analysis of change in the anti-PEG IgM level after injection of PEGylated LNP over time across groups.

Variable	Anti-PEG IgM					
	β (95% CI)	*P*	β (95% CI)	*P*	β (95% CI)	*P*
Group						
Control	0 (ref.)	-	-	-	-	-
L-LNP	0.2337 (-0.0351, 0.5025)	0.0915	0 (ref.)	-	-	-
M-LNP	0.6198 (0.3509, 0.8886)	<0.0001	0.3861 (0.1618, 0.6103)	0.0011	0 (ref.)	-
H-LNP	0.4103 (0.1415, 0.6792)	0.0035	0.1767 (-0.0476, 0.4009)	0.1257	-0.2094 (-0.4336, 0.0148)	0.0701
Time	0.0140 (0.0032, 0.0249)	0.0116	-	-	-	-
Time^2	-0.0008 (-0.0009, -0.0006)	<0.0001	-	-	-	-
Group*Time						
Control*Time	0 (ref.)	-	-	-	-	-
L-LNP*Time	0.0034 (-0.0036, 0.0105)	0.3408	0 (ref.)	-	-	-
M-LNP*Time	0.0238 (0.0167, 0.0308)	<0.0001	0.0203 (0.0145, 0.0262)	<0.0001	0 (ref.)	-
H-LNP*Time	0.0458 (0.0387, 0.0528)	<0.0001	0.0424 (0.0365, 0.0482)	<0.0001	0.0220 (0.0161, 0.0279)	<0.0001
Injection						
First	0 (ref.)	-	-	-	-	-
Second	0.9166 (0.7852, 1.0479)	<0.0001	-	-	-	-

Models considered variables including group, time, time^2, number of injections, and interaction term of group and time as fixed effect and subject as random effect. β for group represents mean differences in antibody levels between groups at all time points. β for time and time^2 represents rate of change in antibody levels over time for the four groups at all time points. β for injection represents mean difference in antibody levels for the four groups at all time points between the first injection and second injection. β for group*time represents mean differences in the rate of change of antibody levels over time between groups. ref: reference.

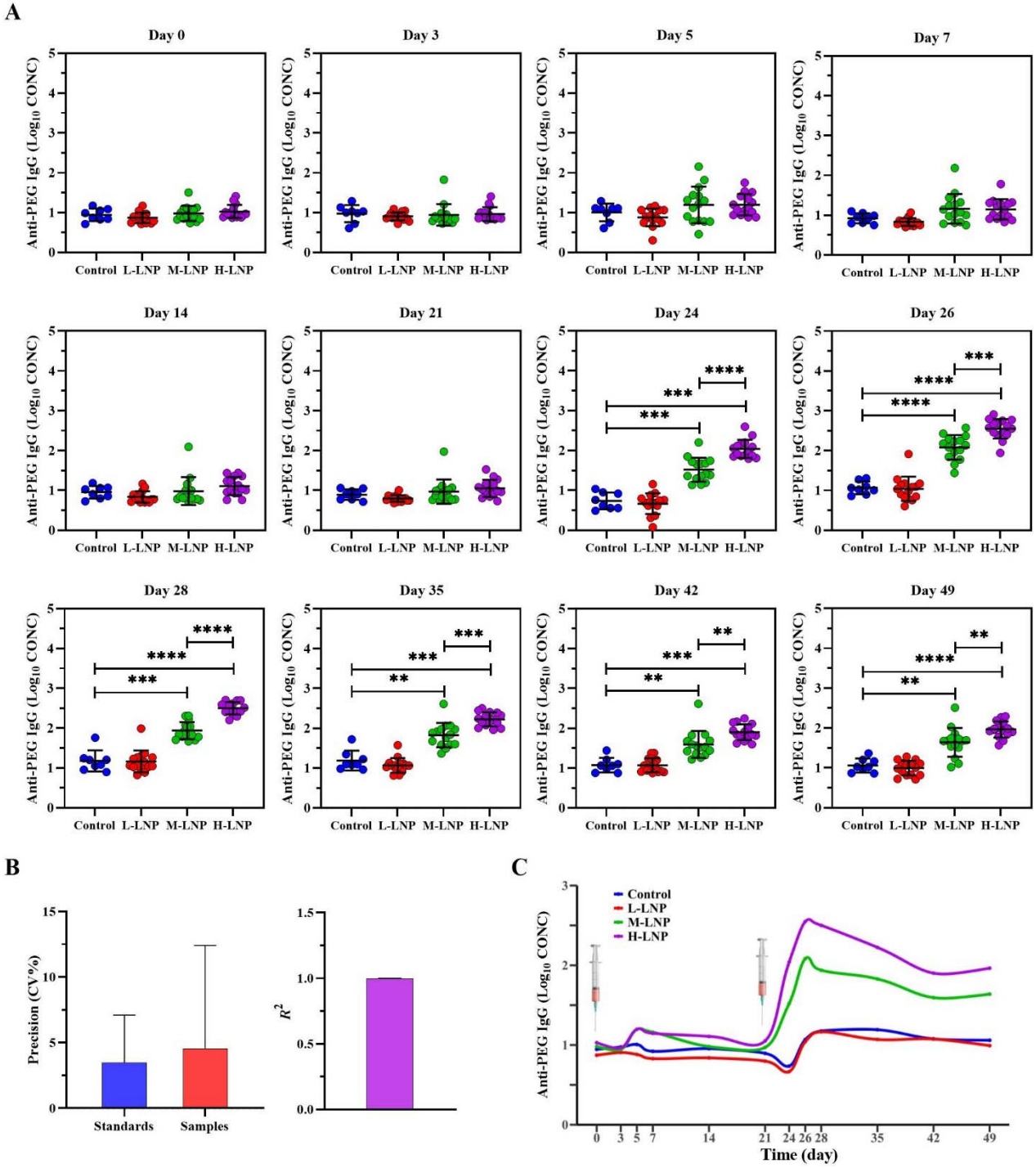

Fig. 4. Evaluation of anti-PEG IgG production in rat. (**A**) Quantitative analysis of anti-PEG IgG (Log_{10} CONC) (log_{10}-transformed concentration of anti-PEG IgG) induced by LNP in rat serum. Data were presented as "mean ± standard deviation", with n=8 for Control group and n=15 for all LNP-treated groups. Differences in anti-PEG IgG (Log_{10} CONC) among various groups were analyzed using Mann-Whitney U test, with *P* values adjusted for FDR (false discovery rate). *, $P<0.05$; **, $P<0.01$; ***, $P<0.001$; ****, $P<0.0001$. (**B**) Excellent quality control of ELISA for determination of anti-PEG IgG. The left image shows the average precision/CV (coefficient of variation) of standards and samples in ELISA, and the right image shows the mean linear regression coefficient of determination of the standard curve for ELISA. (**C**) Time-course of anti-PEG IgG induced by PEGylated LNP. The changing curves of mean anti-PEG IgG (Log_{10} CONC) levels over time were fitted by the R package called "ggalt".

Table 2. Linear mixed model analysis of change in the anti-PEG IgG level after injection of PEGylated LNP over time across groups.

Variable	Anti-PEG IgG					
	β (95% CI)	***P***	**β (95% CI)**	***P***	**β (95% CI)**	***P***
Group						
Control	0 (ref.)	-	-	-	-	-
L-LNP	-0.0950 (-0.2748, 0.0848)	0.3033	0 (ref.)	-	-	-
M-LNP	0.0871 (-0.0927, 0.2669)	0.3449	0.1821 (0.0321, 0.332)	0.0195	0 (ref.)	-
H-LNP	0.1230 (-0.0568, 0.3028)	0.1835	0.2179 (0.068, 0.3679)	0.0054	0.0359 (-0.1141, 0.1858)	0.6404
Time	-0.0092 (-0.0159, -0.0024)	0.0077	-	-	-	-
Time^2	-0.0001 (-0.0002, -0.00002)	0.0197	-	-	-	-
Group*Time						
Control*Time	0 (ref.)	-	-	-	-	-
L-LNP*Time	0.0011 (-0.0033, 0.0054)	0.6339	0 (ref.)	-	-	-
M-LNP*Time	0.0149 (0.0105, 0.0193)	< 0.0001	0.0138 (0.0102, 0.0175)	< 0.0001	0 (ref.)	-
H-LNP*Time	0.0244 (0.0200, 0.0288)	< 0.0001	0.0233 (0.0197, 0.027)	< 0.0001	0.0095 (0.0059, 0.0131)	< 0.0001
Injection						
First	0 (ref.)	-	-	-	-	-
Second	0.6549 (0.5734, 0.7364)	< 0.0001	-	-	-	-

Models considered variables including group, time, time^2, number of injections, and interaction term of group and time as fixed effect and subject as random effect. β for group represents mean differences in antibody levels between groups at all time points. β for time and time^2 represents rate of change in antibody levels over time for the four groups at all time points. β for injection represents mean difference in antibody levels for the four groups at all time points between the first injection and second injection. β for group*time represents mean differences in the rate of change of antibody levels over time between groups. ref: reference.

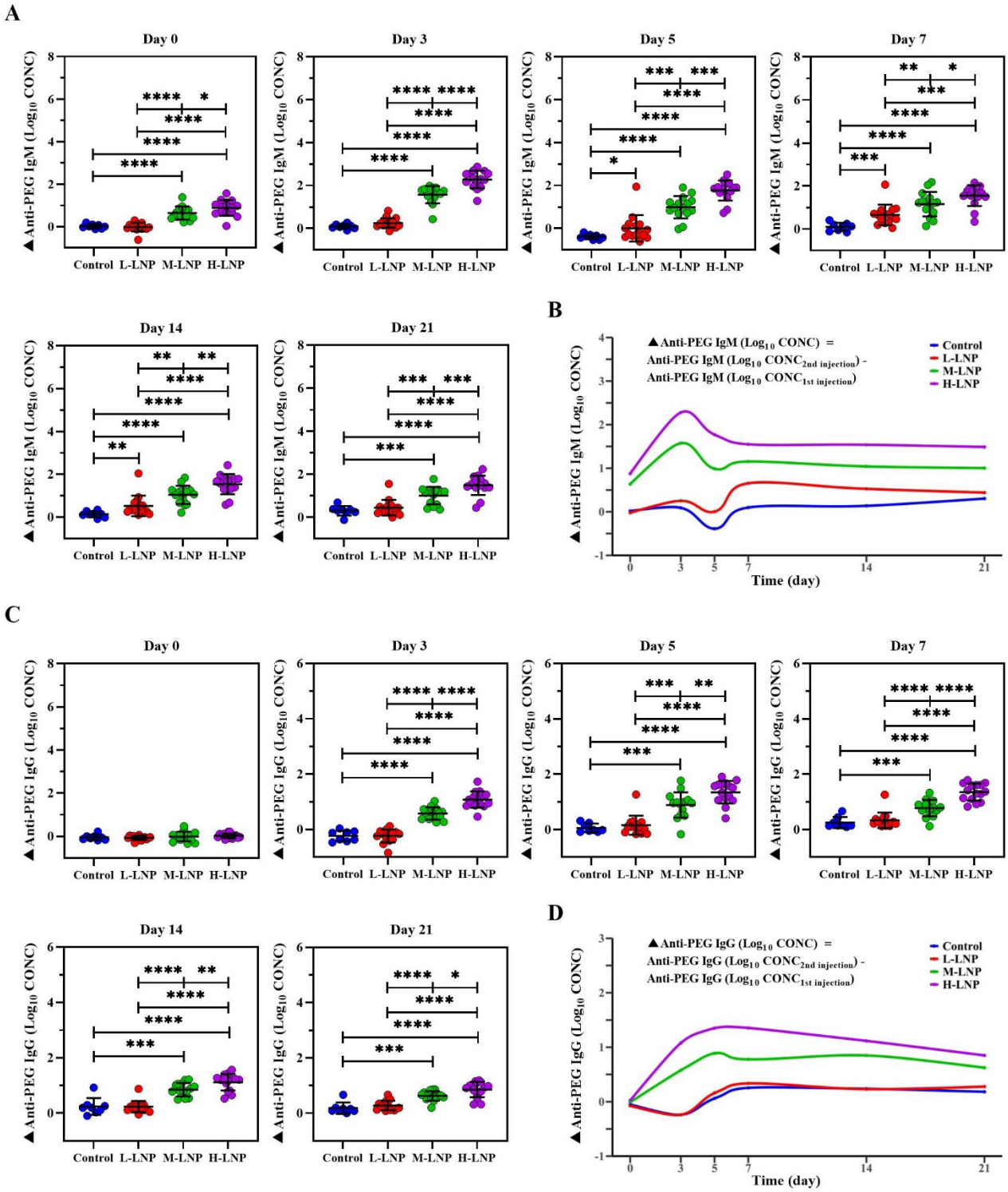

Fig. 5. Enhanced production of anti-PEG antibodies in rat by repeated administration with PEGylated LNP. (**A**) Enhanced anti-PEG IgM production induced by repeated LNP injection. ▲Anti-PEG IgM (Log_{10} CONC) means Anti-PEG IgM (Log_{10} $CONC_{2nd\ injection}$) (log_{10}-transformed concentration of anti-PEG IgM induced during the second injection cycle) subtracted corresponding Anti-PEG IgM (Log_{10} $CONC_{1st\ injection}$) (log_{10}-transformed concentrations of anti-PEG IgM induced during the first injection cycle). (**B**) Time-course of enhanced anti-PEG IgM induced by repeated injection of LNP. (**C**) Enhanced anti-PEG IgG production induced by repeated injection of LNP. ▲Anti-PEG IgG (Log_{10} CONC) means Anti-PEG IgG (Log_{10} $CONC_{2nd\ injection}$) (log10-transformed concentration of anti-PEG IgG induced during the second injection cycle) subtracted corresponding Anti-PEG IgG (Log_{10} $CONC_{1st\ injection}$) (log_{10}-

transformed concentrations of anti-PEG IgG induced during the first injection cycle). (**D**) Time-course of enhanced anti-PEG IgG induced by repeated injection of LNP. In figure **A** and **C**, data were presented as "mean ± standard deviation", with n=8 for Control group and n=15 for all LNP-treated groups. Differences in ▲Anti-PEG IgM (Log_{10} CONC) or ▲Anti-PEG IgG (Log_{10} CONC) among various groups were analyzed using Mann-Whitney U test, with *P* values adjusted for FDR (false discovery rate). *, $P<0.05$; **, $P<0.01$; ***, $P<0.001$; ****, $P<0.0001$. In figure **C** and **D**, changing curves of average level of ▲Anti-PEG IgM (Log_{10} CONC) or ▲Anti-PEG IgG (Log_{10} CONC) over time for various doses were fitted by the R package called "ggalt".

Table 3. Linear mixed model analysis of change in the difference of anti-PEG IgM level (▲Anti-PEG IgM (Log_{10} CONC)) between two injections of PEGylated LNP over time across groups.

Variable	▲Anti-PEG IgM (Log_{10} CONC)					
	β (95% CI)	***P***	**β (95% CI)**	***P***	**β (95% CI)**	***P***
Group						
Control	0 (ref.)	-	-	-	-	-
L-LNP	0.2281 (-0.0915, 0.5477)	0.1653	0 (ref.)	-	-	-
M-LNP	1.1623 (0.8427, 1.4819)	< 0.0001	0.9343 (0.6677, 1.2008)	< 0.0001	0 (ref.)	-
H-LNP	1.6775 (1.3579, 1.9971)	< 0.0001	1.4494 (1.1828, 1.716)	< 0.0001	0.5152 (0.2486, 0.7817)	0.0003
Time	0.0725 (0.0441, 0.1009)	< 0.0001	-	-	-	-
$Time^2$	-0.0026 (-0.0037, -0.0015)	< 0.0001	-	-	-	-
Group*Time						
Control*Time	0 (ref.)	-	-	-	-	-
L-LNP*Time	0.0045 (-0.0156, 0.0247)	0.6596	0 (ref.)	-	-	-
M-LNP*Time	-0.0167 (-0.0369, 0.0034)	0.1048	-0.0213 (-0.0381, -0.0045)	0.0138	0 (ref.)	-
H-LNP*Time	-0.0165 (-0.0367, 0.0037)	0.1099	-0.021 (-0.0379, -0.0042)	0.0149	0.0002 (-0.0166, 0.0171)	0.9775

Models considered variables including group, time, $time^2$, and interaction term of group and time as fixed effect and subject as random effect. β for group represents mean differences in the average levels of ▲Anti-PEG IgM (Log_{10} CONC) among groups at all time points. β for time and $time^2$ represents change rate in ▲Anti-PEG IgM (Log_{10} CONC) over time for the four groups at all time points. β for group*time represents mean differences in the change rates of ▲Anti-PEG IgM (Log_{10} CONC) over time between groups. ▲Anti-PEG IgM (Log_{10} CONC) was defined as Anti-PEG IgM (Log_{10} $CONC_{2nd\ injection}$) (log_{10}-transformed concentration of anti-PEG IgM induced during the second injection cycle) subtracting corresponding Anti-PEG IgM (Log_{10} $CONC_{1st\ injection}$) (log_{10}-transformed concentrations of anti-PEG IgM induced during the first injection cycle). ref: reference.

Table 4. Linear mixed model analysis of change in the difference of anti-PEG IgG level (▲Anti-PEG IgG (Log_{10} CONC)) between two injections of PEGylated LNP over time across groups.

Variable	▲Anti-PEG IgG (Log_{10} CONC)					
	β (95% CI)	*P*	β (95% CI)	*P*	β (95% CI)	*P*
Group						
Control	0 (ref.)	-	-	-	-	-
L-LNP	0.0149 (-0.1866, 0.2164)	0.8847	0 (ref.)	-	-	-
M-LNP	0.5180 (0.3165, 0.7195)	< 0.0001	0.503 (0.335, 0.6711)	< 0.0001	0 (ref.)	-
H-LNP	0.8861 (0.6846, 1.0876)	< 0.0001	0.8711 (0.7031, 1.0392)	< 0.0001	0.3681 (0.2, 0.5362)	< 0.0001
Time	0.1232 (0.1022, 0.1442)	< 0.0001	-	-	-	-
$Time^2$	-0.0050 (-0.0058, -0.0042)	< 0.0001	-	-	-	-
Group*Time						
Control*Time	0 (ref.)	-	-	-	-	-
L-LNP*Time	0.0031 (-0.0118, 0.0180)	0.6848	0 (ref.)	-	-	-
M-LNP*Time	0.0030 (-0.0119, 0.0179)	0.6899	-0.0001 (-0.0125, 0.0124)	0.9933	0 (ref.)	-
H-LNP*Time	0.0002 (-0.0147, 0.0151)	0.9832	-0.0029 (-0.0154, 0.0095)	0.6445	-0.0029 (-0.0153, 0.0096)	0.6505

Models considered variables including group, time, $time^2$, and interaction term of group and time as fixed effect and subject as random effect. β for group represents mean differences in the average levels of ▲Anti-PEG IgG (Log_{10} CONC) among groups at all time points. β for time and $time^2$ represents change rate in ▲Anti-PEG IgG (Log_{10} CONC) over time for the four groups at all time points. β for group*time represents mean differences in the change rates of ▲Anti-PEG IgG (Log_{10} CONC) over time between groups. ▲Anti-PEG IgG (Log_{10} CONC) was defined as Anti-PEG IgG (Log_{10} $CONC_{2nd\ injection}$) (log_{10}-transformed concentration of anti-PEG IgG induced during the second injection cycle) subtracting corresponding Anti-PEG IgG (Log_{10} $CONC_{1st\ injection}$) (log_{10}-transformed concentrations of anti-PEG IgG induced during the first injection cycle). ref: reference.

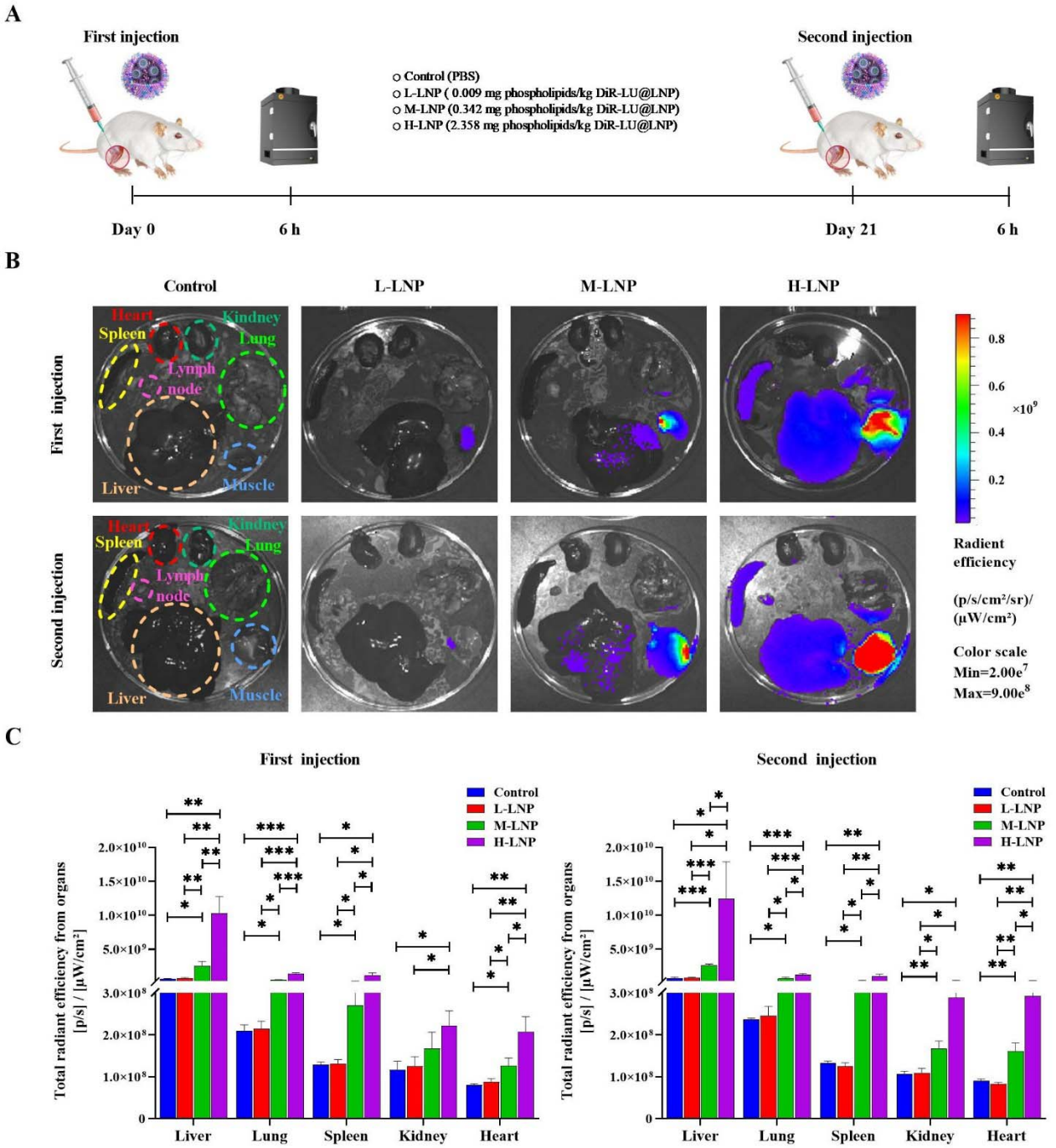

Fig. 6. Experimental design and biodistribution of PEGylated LNP in representative organs of rat. (**A**) Schematic illustration of the experimental protocols. Wistar rats were injected intramuscularly with 0.009 (L-LNP group), 0.342 (M-LNP group) or 2.358 (H-LNP) mg phospholipids/kg DiR-LU@LNP on Day 0 and Day 21, respectively. Rats in the Control group were injected with PBS. Six hours after each injection, three rats from each experimental group were sacrificed and immediately dissected. Major organs including heart, liver, spleen, lung, kidneys and draining lymph node, and muscle at the injection site were collected for fluorescence imaging with IVIS Spectrum imaging system. (**B**) Representative fluorescence images of major organs and muscle tissues isolated from rats 6 hours after the first and second injection of DiR-LU@LNP. (**C**) Total radiant efficiency of major organs determined 6 hours after the first and second injection of DiR-LU@LNP. Data were presented as "mean ± standard deviation" (n=3). Differences in total radiation efficiency induced by three doses were analyzed using multiple unpaired *t* tests with correction for multiple testing. *, $P<0.05$; **, $P<0.01$; ***, $P<0.001$; ****,

946 $P<0.0001$.

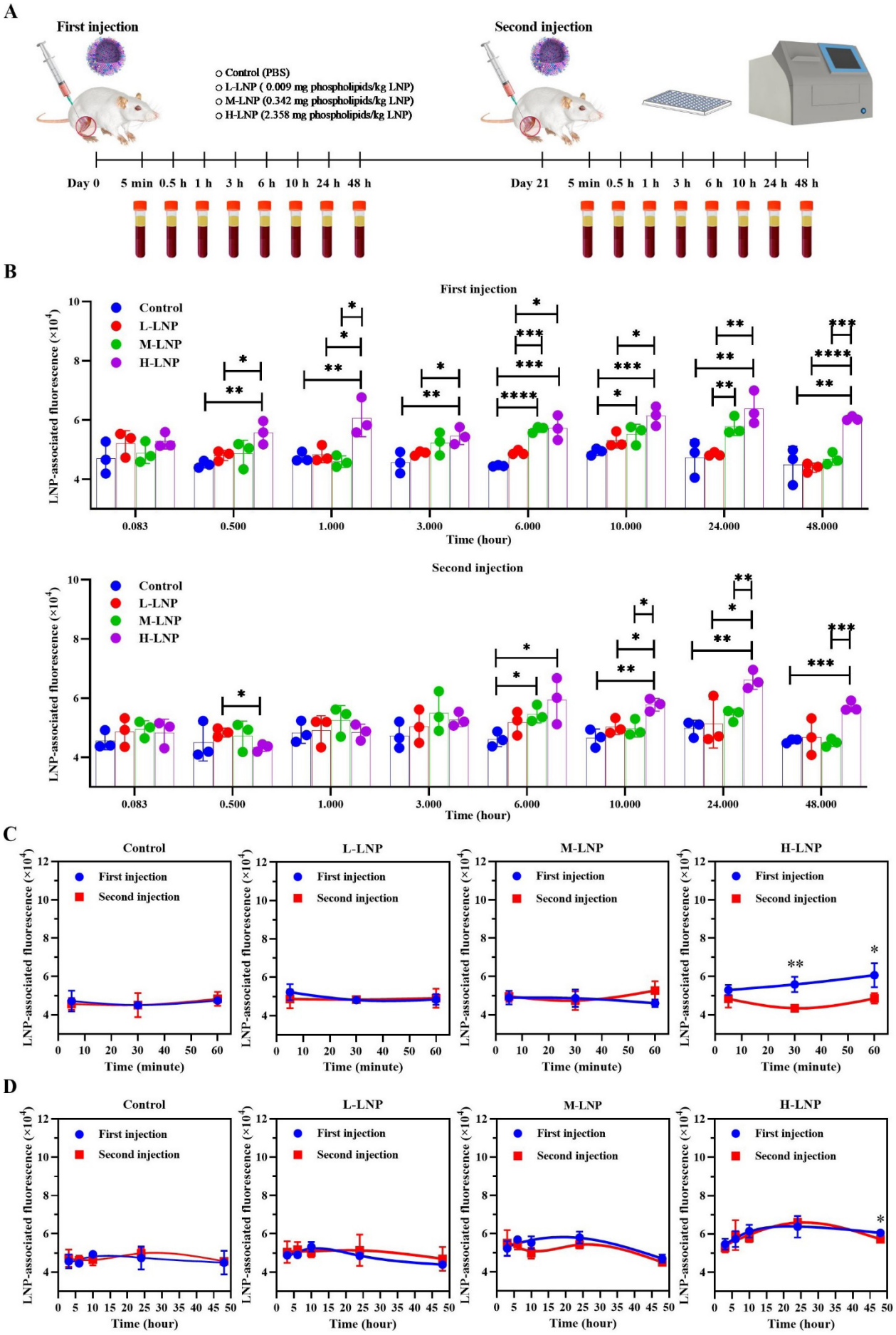
A
First injection
Second injection
Control (PBS)
L-LNP (0.009 mg phospholipids/kg LNP)
M-LNP (0.342 mg phospholipids/kg LNP)
H-LNP (2.358 mg phospholipids/kg LNP)
Day 0
5 min 0.5 h 1 h 3 h 6 h 10 h 24 h 48 h
Day 21
5 min 0.5 h 1 h 3 h 6 h 10 h 24 h 48 h
B
First injection
Second injection
Control
L-LNP
M-LNP
H-LNP
LNP-associated fluorescence (×10^4)
Time (hour)
0.083
0.500
1.000
3.000
6.000
10.000
24.000
48.000
C
Control
L-LNP
M-LNP
H-LNP
First injection
Second injection
LNP-associated fluorescence (×10^4)
Time (minute)
D
Control
L-LNP
M-LNP
H-LNP
First injection
Second injection
LNP-associated fluorescence (×10^4)
Time (hour)

Fig. 7. Experimental design and blood clearance of PEGylated LNP in rats. (**A**) Schematic illustration of the experimental protocols. Wistar rats were injected intramuscularly with 0.009 (L-LNP group), 0.342 (M-LNP group) or 2.358 (H-LNP) mg phospholipids/kg DiR-LNP on Day 0 and Day 21, respectively. Rats in the Control group were injected with PBS. Serum samples were collected at the indicated 8 time points (5 minutes, 30 minutes, 1 hour, 3 hours, 6 hours, 10 hours, 24 hours and 48 hours) after each injection of DiR-LNP, followed by determination of LNP-associated fluorescence with Spectramax ID5 fluorescent spectrometry. (**B**) LNP-associated fluorescence was presented as "mean ± standard deviation" (n=3) for each group, with differences among various groups after each injection analyzed using the multiple unpaired *t* test, with *P* values adjusted for FDR (false discovery rate). *, $P<0.05$; **, $P<0.01$; ***, $P<0.001$; ****, $P<0.0001$. (**C**) Blood clearance profile of DiR-LNP in rats based on LNP-associated fluorescence obtained at 5 minutes, 30 minutes and 1 hour, with fitted curves created by Prism 9.2.0 (GraphPad Software). (**D**) Blood clearance profile of DiR-LNP in rats based on LNP-associated fluorescence obtained at 3 hours, 6 hours, 10 hours, 24 hours and 48 hours, with fitted curves created by Prism 9.2.0 (GraphPad Software). As the earliest three time points presented in **C** would become invisible if combined with 5 later time points, blood clearance profile of DiR-LNP based on all 8 time points was presented as two parts (**C** and **D**). Data in **C** and **D** were presented as "mean ± standard deviation" (n=3) for each group, with differences between two injections analyzed using the multiple unpaired *t* test, with *P* values adjusted for FDR (false discovery rate). *, $P<0.05$; **, $P<0.01$; ***, $P<0.001$; ****, $P<0.0001$.